eLife

Reviewed Preprint
v1 • May 15, 2026
Not revised

For correspondence:
ez225@cam.ac.uk
skotheim@stanford.edu

Competing interests: No competing interests declared

Funding: See page 21

Reviewing editor: Alexis Barr, MRC Laboratory of Medical Sciences, United Kingdom

Cell size modulates ferroptosis susceptibility

Evgeny Zatulovskiy[1,2], Magdalena B Murray[2], Shuyuan Zhang[2], Scott J Dixon[2], Jan M Skotheim[2,3]

[1]Department of Biochemistry, University of Cambridge, Cambridge, United Kingdom • [2]Department of Biology, Stanford University, Stanford, United States • [3]Chan-Zuckerberg Biohub, Stanford, United States

eLife Assessment

This **important** study highlights how cell size influences various cellular responses, with a particular focus on ferroptosis. The evidence presented is **convincing**, employing multiple model systems and experimental approaches to support the conclusions. This work will be of significant interest to the fields of cell size, ferroptosis, and cancer biology.

[Editors' note: this paper was reviewed by *Review Commons*.]

https://doi.org/10.7554/eLife.111544.1.sa4

Abstract

Size is a fundamental property of cells that influences many aspects of their physiology. This is because cell size sets the scale for all subcellular components and drives changes in the composition of the proteome. Given that large and small cells differ in their biochemical composition, we hypothesize that they should also differ in how they respond to signals and make decisions. Here, we investigated how cell size affects susceptibility to cell death. We found that large cells are more resistant to ferroptosis caused by system x_c^- inhibition. Ferroptosis is a type of cell death characterized by the iron-dependent accumulation of toxic lipid peroxides. This process is opposed by cysteine-dependent lipid peroxide detoxification mechanisms. We found that larger cells exhibit higher concentrations of the cysteine-containing metabolite glutathione and lower concentrations of membrane lipid peroxides. Mechanistically, this can be explained by the fact that larger cells had lower concentrations of an enzyme that enriches cellular membranes with peroxidation-prone polyunsaturated fatty acids, ACSL4, and increased concentrations of the iron-chelating protein ferritin, the glutathione-producing enzymes glutamate-cysteine ligase and glutathione synthetase, and the lysosomal protease cathepsin B, which can catabolize cysteine-rich extracellular proteins to produce additional cystine for fueling the synthesis of glutathione. Taken together, our results highlight the significant impact of cell size on cellular function and survival, revealing a size-dependent vulnerability to ferroptosis that could influence therapeutic strategies based on this cell death pathway.

Introduction

Cell size is fundamental to cell physiology. This is because it impacts cell geometry and sets the scale of all biosynthetic processes in the cell (Chan & Marshall, 2010; Ginzberg et al, 2015; Zatulovskiy & Skotheim, 2020). The importance of cell size is most clearly seen when yeast and mammalian cells become excessively large. In these cases, cells are not able to maintain optimal protein and mRNA concentrations to support growth as their cytoplasm becomes more dilute, unless the increase in cell size is coulter-balanced by the increase in cell ploidy (Neurohr et al, 2019; Lanz et al, 2022, 2024; Zatulovskiy et al, 2022). Such excessively large cells exhibit features of senescence and are no longer able to enter the cell division cycle. Unsurprisingly, cell size regulation is compromised in many diseases and during aging (Sandlin et al, 2022; Nguyen et al, 2016; Lengefeld et al, 2021). As animals, including humans, grow older, they contain more 'senescent' cells that tend to be larger (Davies et al, 2022). For example, basal keratinocytes

are about 1.5 times as large when humans are 80 years old versus 20 (Liao et al, 2012). Conversely, cancer cells often exhibit an extreme heterogeneity in cell size, which may be associated with more proliferation (Sandlin et al, 2022; Nguyen et al, 2016; Li et al, 2015; Bell & Waizbard, 1986). Taken together, these studies argue for the importance of cell size in both natural and disease contexts.

Due to the importance of cell size for cell physiology, this property is highly regulated by distinct classes of molecular mechanisms. One class of mechanisms regulates the cell growth rate so that smaller cells grow faster and add proportionally more biomass than larger cells within one cell division cycle to ensure that all cells divide at similar sizes (Ginzberg et al, 2018; Liu et al, 2024; Conlon & Raff, 2003). A second class of molecular mechanisms, useful in more regular shaped cell types like rod shaped bacteria and fission yeast, relies on geometrical parameters such as cell length or surface area to measure cell size and determine that appropriate timing for initiating cell division (Miller et al, 2023; Martin & Berthelot-Grosjean, 2009; Pan et al, 2014; Bhatia et al, 2014; Moseley & Nurse, 2010). Finally, a third class of mechanisms rely on differential changes in protein concentrations of cell cycle activators and cell cycle inhibitors as cells grow larger (Chen et al, 2020b; Zatulovskiy et al, 2020; Schmoller et al, 2015). Typically, cell cycle activators either remain at constant concentration or increase with cell size, while some key cell cycle inhibitors, like the transcriptional inhibitors Whi5 in budding yeast and the retinoblastoma protein RB in human cells, are progressively diluted in larger cells to trigger their division (Zatulovskiy et al, 2020; Schmoller et al, 2015; Zhang et al, 2022b, 2024).

That some larger cells initiate division through increases in the concentrations of cell cycle activators relative to cell cycle inhibitors was surprising because previous bulk studies showed that total protein concentration remained constant as cells grew larger. However, this constant concentration of total protein masked changes in the concentrations of individual proteins as cells grow larger, as revealed by a systematic quantitative proteomics analysis (Lanz et al, 2022, 2024; Zatulovskiy et al, 2022). The proteomics analyses revealed that as cell size increases, the concentrations of numerous senescence-related proteins begin to approach those of a senescent cell, even before cells lose the ability to enter the cell division cycle (Lanz et al, 2022; Crozier et al, 2023). This may in part explain the association of large cell size with the senescent state. Moreover, large cells have difficulty in replicating and repairing their genomes, which may be related to the lower concentrations of DNA replication and repair enzymes observed in larger cells (Lanz et al, 2022; Crozier et al, 2022; Manohar et al, 2023; Foy et al, 2023; Wilson et al, 2023). Taken together, these results indicate that a cell size increase in the absence of DNA replication impacts cell physiology through changing the composition of the proteome.

If cell size drives widespread changes in proteome composition, then this might impact many areas of cell physiology, including the susceptibility to cell death. Indeed, proteomic and transcriptomic comparisons of different-sized cells within the same cell type identified concentration changes for many genes involved in regulated cell death (Lanz et al, 2022; Miettinen & Björklund, 2016). Consistent with this, cell size is correlated with some cell death decisions – smaller cells have a higher likelihood to undergo apoptosis both in cell cultures and during *C. elegans* and *D. melanogaster* development (Miettinen & Björklund, 2016; Sethi et al, 2022; Kiyomitsu & Cheeseman, 2013; Hatzold & Conradt, 2008; Chen et al, 2016; Cordes et al, 2006). Inspired by these studies, we aimed to mechanistically investigate how cell size affects different cell death responses in human cells, as it remains unknown whether cell size impacts non-apoptotic cell death.

To test if there is a relationship between cell size and cell death, we used a high-throughput microscopy based approach to examine a variety of stresses (Forcina et al, 2017; Inde et al, 2020). We found that susceptibility to ferroptosis, an iron-dependent form of cell death, demonstrated the strongest dependence on cell size. This finding resonates with a recent report that cell susceptibility to RSL3, a chemical that induces ferroptosis by inhibiting the reduction of lipid peroxides by glutathione peroxidase 4 (GPX4), increases with cell size (Chan et al, 2025). Inhibition of the cystine/glutamate antiporter system x_c^-, using the small molecule erastin2 (Era2) (Dixon et al, 2014) preferentially induced cell death in smaller cells, while larger cells were

more resistant. Ferroptosis is characterized by the accumulation of toxic lipid peroxides (Jiang et al, 2021; Dixon & Olzmann, 2024). To suppress this accumulation and prevent ferroptosis, cells can use cystine/cysteine-derived metabolites, like the reduced tripeptide glutathione (GSH), to prevent the accumulation of peroxidized lipids. The lower susceptibility of large cells to Era2-induced ferroptosis can likely be explained by our observation that larger cells are able to produce higher amounts of GSH per unit protein mass, and that they have a lower concentration of enzymes like ACSL4 that incorporate oxidizable polyunsaturated fatty acids into the plasma membrane (Doll et al, 2017). Supporting this model, the genetic disruption of *ACSL4* reduced the size dependence of lipid peroxidation and ferroptotic cell death. Taken together, our results show how large cell size can protect against ferroptosis.

Results

Larger cells are less susceptible to ferroptosis

To test our hypothesis that cell size affects susceptibility to cell death, we exposed cells of different sizes to a variety of compounds known to induce different forms of cell death. To do this, we first used fluorescence-activated cell sorting (FACS) to isolate small and large G1-phase HMEC-*hTERT* cells (human mammary epithelium cells immortalized with telomerase, herein referred to as HMEC for brevity) (Fig. 1A,B) (Lanz et al, 2022). We sorted cells for size using side scatter, which correlates well with cell size (Lanz et al, 2022; Tzur et al, 2011; Berenson et al, 2019). In this experiment we used DNA staining with Hoechst dye to only collect the cells that were in G1 phase of the cell cycle, since the cell cycle phase can influence cell survival (Rodencal et al, 2024; Ruiz-Losada et al, 2022; Lee et al, 2024; Kuganesan et al, 2023). The small- and large-sorted cells were then seeded into 384-well plates and treated with death-inducing compounds over a range of different doses. Each population of cells was then monitored using high-throughput fluorescence microscopy for 72 h to measure dose-dependent responses and cell death kinetics (Forcina et al, 2017; Inde et al, 2020).

Comparing dose-response curves for small and large cells across different compounds, we observed the largest size-dependent differences in cell death susceptibility in response to erastin2 (Era2). Era2 induces ferroptosis by inhibiting system x_c^- (Dixon et al, 2014). Larger HMEC cells were resistant to higher doses of Era2 than smaller cells. For example, at the 72 h time point, the Era2 IC_{50} was 28 ± 11 μM (mean ± SD) for large cells versus 2.0 ± 1.4 μM for small cells (Student's t-test: $p = 0.039$) (Fig. 1C). Moreover, larger cells exhibit slower cell death kinetics (Fig. 1D). By contrast, for compounds that cause cell death by disrupting protein synthesis (puromycin, anisomycin), inducing DNA damage (doxorubicin), inhibiting protein glycosylation (tunicamycin), or blocking proteasome function (bortezomib), IC_{50} values were not statistically significantly different for large versus small cells (Fig. 1E). We note that this does not eliminate the possibility that there are size-dependent differences in susceptibilities to these compounds that would manifest if our size range were expanded further. However, since the most pronounced differences were observed for Era2, we focused our investigation on how cell size affects ferroptosis.

To test if protection against ferroptosis by large cell size was generalizable beyond HMEC cells isolated by FACS, we used alternative methods to generate different sized populations of cells and tested additional cell lines. We examined the HT-1080 fibrosarcoma cell line, commonly used in ferroptosis studies (Dixon et al, 2012), and non-transformed telomerase-immortalized retinal pigment epithelium cells (RPE-1 cell line), commonly used in cell cycle and cell size studies. We used FACS to sort G1-phase HT-1080 cells into four cell size bins and treated these cells with 0.3 μM Era2. As observed in HMEC cells, larger HT-1080 and RPE-1 cells were more resistant to ferroptotic cell death (Fig. S1A). Next, to generate populations of different-sized cells without cell sorting, we arrested HT-1080 cells in early G1 using the cell-cycle inhibitor palbociclib (CDK4/6 inhibitor) for 2-6 days (Neurohr et al, 2019; Lanz et al, 2022; Crozier et al, 2023; Manohar et al, 2023; Foy et al, 2023). Larger cells, which were arrested in G1 for a longer time, were less sensitive to Era2 than smaller cells arrested for a shorter duration (Fig. 2A,B). We note that non-arrested cells had a lower susceptibility to Era2-induced ferroptosis compared to cells that were arrested in

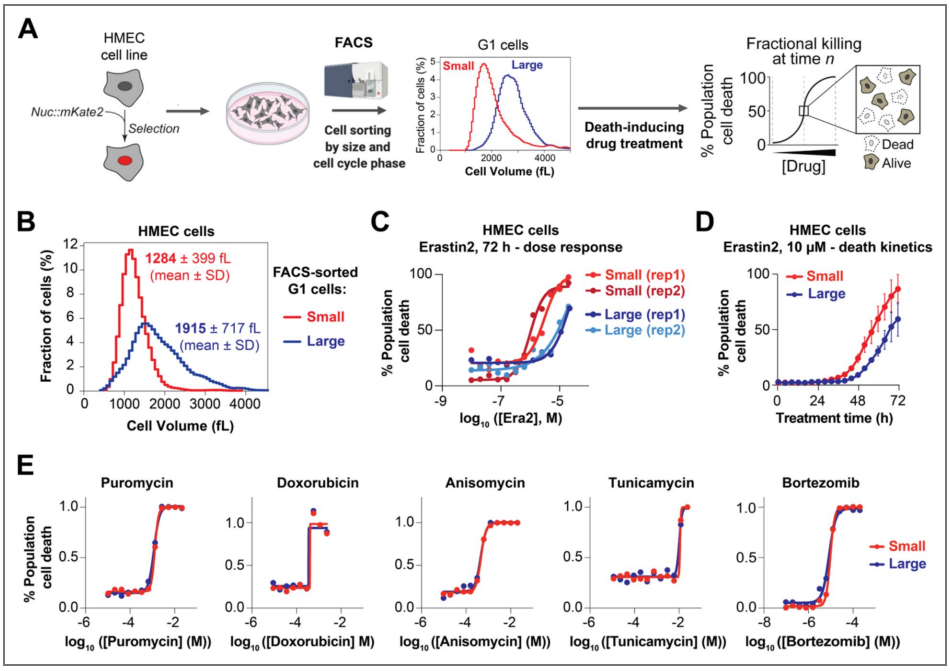

Figure 1. High-throughput microscopy-based measurement of cell death susceptibility in different-sized cells.

(A) Experiment schematic: a genetic construct encoding nuclear-localized fluorescent protein mKate2 was delivered into HMEC cells using lentiviral transduction. After selection, these cells were FACS-sorted by cell cycle phase and cell size into small and large G1 cells (smallest and largest 5%). The FACS-sorted cells were seeded on 384-well plates and allowed to settle overnight before being treated with death-inducing compounds in the media containing a dead-cell dye SYTOX Green. The cells were imaged for 72 h during treatment, and live cells were identified by the presence of nuclear mKate2 fluorescence, while dead cells were identified by the presence of the SYTOX Green signal (Forcina et al, 2017; Inde et al, 2020). The numbers of live and dead cells were automatically tracked over time to determine the dose-response curves and cell death kinetics. (B) Cell size distributions of small and large G1-phase HMEC cells after FACS sorting, measured on a Coulter counter. (C) Dose-response curves of small and large FACS-sorted HMEC cells treated with a potent ferroptosis-inducing compound erastin2 (Era2). Rep1 and rep2 denote two different biological replicates, each with two technical replicates. (D) Cell death kinetics of small and large FACS-sorted HMEC cells treated with 10 µM Era2. Dots show the means of two biological replicates, error bars denote the range. (E) Dose-response curves of small and large FACS-sorted HMEC cells treated for 72 h with other lethal compounds: puromycin, doxorubicin, anisomycin, tunicamycin and bortezomib. Each experiment was performed twice independently, and each biological replicate included two technical replicates. The dots show averages of two biological replicates.

G1 for 2-3 days, despite being smaller in size. This is likely due to the difference in the fraction of cells in different cell cycle phases between arrested and non-arrested conditions since cells in S/G2/M phases are known to be more resistant to ferroptosis than cells in G0/G1 phases (Rodencal et al, 2024; Kuganesan et al, 2023).

We further confirmed that the effects of cell size on Era2-induced ferroptosis susceptibility are generalizable across cell lines and independent of the cell cycle. To do this, we treated RPE1 cells with palbociclib for 2 or 4 days and then measured their susceptibility to Era2. Both the cells treated with palbociclib for 2 days and for 4 days were arrested in G1, but the cells treated for 4 days were nearly two-fold larger than the cells treated for 2 days (Fig 2C,D). This enabled us to isolate the effects of cell size from cell cycle effects and confirm that larger cells were significantly more resistant to Era2-induced ferroptosis compared to their smaller counterparts in the same phase of the cell cycle (Fig 2E).

As an additional means to generate populations of different sized cells, we used inducible shRNA-mediated cyclin D1 (*CCND1*) knockdown in RPE-1 cells to generate a population of cells that had larger cell sizes compared to uninduced RPE-1 cells (You et al, 2025). As previously reported, cells that inducibly expressed *CCND1* shRNA had a ~30% decrease in Cyclin D1 protein concentration but continued to grow and proliferate, though at a lower division rate (You et al, 2025). As a result, these *CCND1* knockdown cells were larger than uninduced cells, and were less susceptible to Era2 (Fig. 2F,G).

Our finding that larger cells are less susceptible to ferroptosis induced by Era2 treatment seemingly contradicted findings that large size sensitizes cells to the ferroptosis-inducing compound RSL3 (Chan et al, 2025). Unlike Era2, which acts by inhibiting cystine/glutamate antiporter system x_c^- and thereby depleting glutathione (GSH) pool, RSL3 belongs to a different class of ferroptosis inducers, which acts by inhibiting glutathione peroxidase 4 (GPX4) (Yang et al, 2014), a key enzyme that uses GSH to reduce toxic lipid peroxidation. To compare the effects of these two classes of compounds in our experimental system, we treated the HT-1080 cells, arrested in G1 for 2-6 days using palbociclib, with RSL3 (Fig. S1B). Consistent with the published report (Chan et al, 2025) and in contrast to Era2 treatment (Fig. 2B), increased cell size during G1 arrest progressively increased sensitivity to RSL3. This difference in cell responses to the two different classes of ferroptosis inducers has been noted in several reports describing context-dependent responses to different classes of ferroptosis inducers (Chan et al, 2025; Rodencal et al, 2024; Magtanong et al, 2022).

Taken together, our measurements demonstrate that in human cell cultures, larger cells are generally less susceptible to ferroptosis induced by system x_c^- inhibition (Fig. 2H). We observed this result in populations of different sized cells that were generated through multiple methods including genetics, FACS sorting, and small molecule-induced cell cycle arrest.

Membrane lipid peroxidation decreases with cell size

Ferroptosis is defined and caused by the accumulation of toxic products from polyunsaturated fatty acid (PUFA) peroxidation in the plasma membrane (Jiang et al, 2021; Dixon & Olzmann, 2024) (Fig. 3A). We therefore next sought to determine how cell size affects ferroptosis-associated lipid peroxidation. Lipid peroxidation can be detected using a ratiometric fluorescent sensor dye BODIPY-C11 581/591 (Dixon et al, 2012; Pap et al, 1999). This dye can be used for ratiometric analysis of lipid peroxidation in flow cytometry, which detects a shift of the fluorescence emission peak from red (~590 nm) to green (~510 nm) caused by the oxidation of the polyunsaturated butadienyl portion of this fatty acid analog. When HMEC cells are treated with Era2, which leads to increased lipid peroxidation, we find a decrease in non-oxidized (red) BODIPY-C11 fluorescence and an increase in oxidized (green) BODIPY-C11 as expected (Fig. 3B).

To determine how cell size affects basal lipid peroxidation in cells, we first stained control (DMSO-treated) cells with BODIPY-C11 and subjected them to a flow cytometry analysis using side scatter (SSC-A) as a proxy for cell size (Lanz et al, 2022; Tzur et al, 2011). When we plotted the oxidized to non-oxidized BODIPY-C11 ratio against cell size, we observed a clear anti-correlation

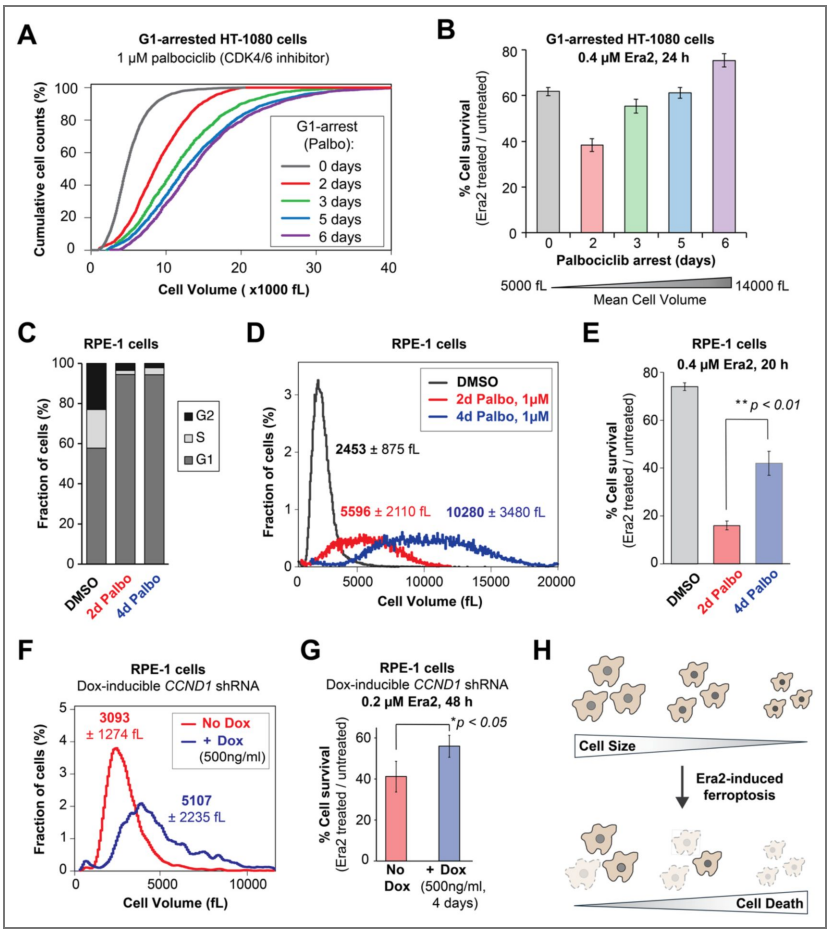

Figure 2. Larger cells are less susceptible to Era2-induced ferroptosis.

(A) Cumulative cell size distributions of HT-1080 cells, whose cell cycle was arrested in G1 phase for 0, 2, 3, 5, or 6 days with 1 μM of the CDK4/6 inhibitor palbociclib. (B) Cell survival percentage of HT-1080 cells whose size was increased through palbociclib-induced cell cycle arrest. After pre-treatment with palbociclib for the indicated numbers of days, the cells were exposed to 0.4 μM Era2 in the presence of palbociclib for 24 h. Cell survival percentage was calculated relative to the cells treated only with palbociclib. (C) Cell cycle phase distribution of asynchronously proliferating RPE-1 cells, and RPE-1 cells treated with the CDK4/6 inhibitor palbociclib for 2 or 4 days. (D) Cell size distribution of asynchronously proliferating RPE-1 cells, and RPE-1 cells treated with the CDK4/6 inhibitor palbociclib for 2 or 4 days. The numbers next to the histograms indicate mean cell size ± standard deviation for the corresponding condition. (E) Cell survival percentage in RPE-1 cells whose cell cycle was synchronized and size was increased through 2-day or 4-day palbociclib-induced cell cycle arrest. After pre-treatment with palbociclib for the indicated numbers of days, the cells were exposed to 0.4 μM Era2 in the presence of palbociclib for 20 h. Cell survival percentage was calculated relative to the cells treated only with palbociclib. (F) Cell size distributions of RPE-1 cells that inducibly express shRNA against cyclin D1 gene (*CCND1*) to slow down the cell cycle and increase cell size. Cells were grown in medium containing 500 ng/mL doxycycline for 4 days to induce shRNA expression and increase cell size. Uninduced cells were grown in the same medium with DMSO in place of doxycycline. (G) Cell survival percentage in control RPE-1 cells and cells expressing an shRNA against cyclin D1 gene (*CCND1*). Cells were treated with 0.2 μM Era2 for 48 h, and cell survival percentage was calculated relative to DMSO-treated cells. Cell survival percentages in graphs (B), (E) and (G) are shown as means ± s.e.m.; n = 3 biological replicates. A two-tailed unpaired Student's t-test was used to evaluate the statistical significance of survival percentage differences in panels (E) and (G). (H) Graphical summary: Larger cells are less susceptible to Era2-induced ferroptosis.

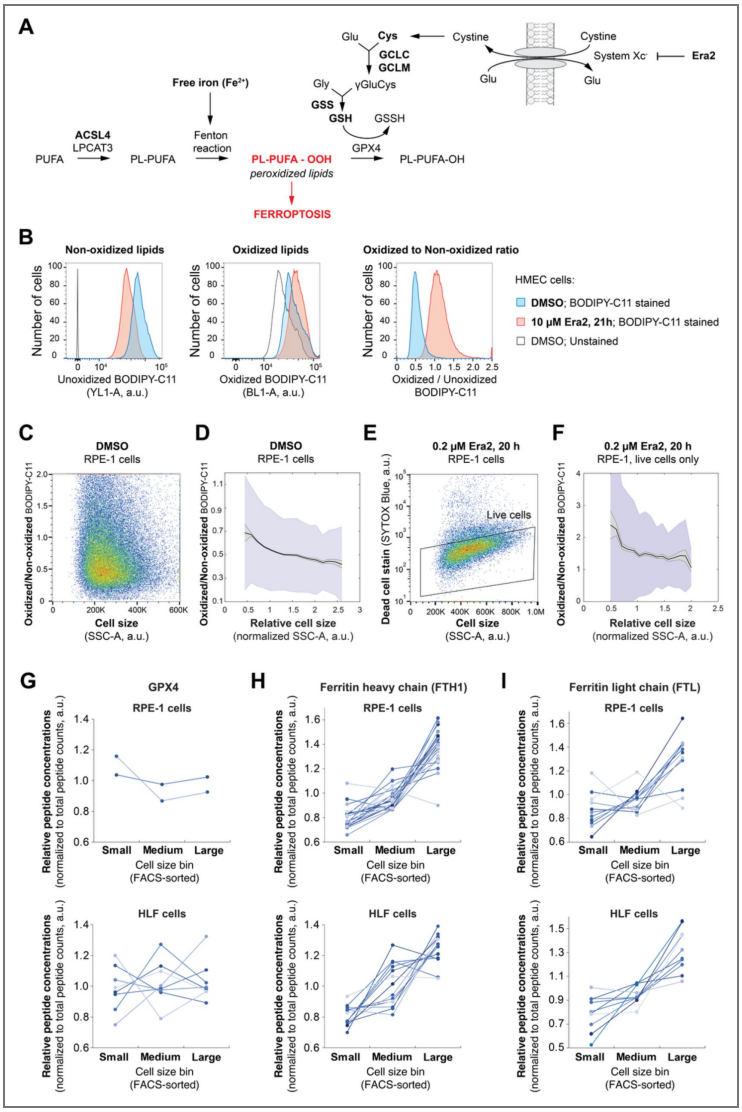

Figure 3. Membrane lipid peroxidation decreases with cell size.

(A) Schematic of pathways regulating ferroptosis. Ferroptosis is induced through the accumulation of toxic peroxidized lipid species in the plasma membrane. The accumulation of peroxidized lipids is prevented by glutathione (GSH) production and GSH-dependent reduction of the peroxidized lipids (Jiang et al, 2021; Dixon & Olzmann, 2024). (B) The ratiometric fluorescent dye BODIPY-C11 581/591 detects lipid peroxidation in live HMEC cells (Dixon et al, 2012; Pap et al, 1999). Oxidation of the polyunsaturated butadienyl portion of this fatty acid analog results in a shift of the fluorescence emission peak from red (~590 nm) to green (~510 nm), allowing ratiometric analysis of lipid peroxidation using flow cytometry. Treatment of cells with Era2 increases lipid peroxidation, as indicated by decreased non-oxidized (red) BODIPY-C11 fluorescence and increased oxidized (green) BODIPY-C11 fluorescence. (C) A flow cytometry analysis of lipid peroxidation in different-sized RPE-1 cells within the DMSO-treated cell culture. The side-scatter parameter (SSC-A) was used as a proxy for cell size (Lanz et al, 2022; Tzur et al, 2011). Three biological replicates were performed, and 100,000 events were recorded for each. (D) A quantitative analysis of the flow cytometry data from panel (C): the data were binned into 12 bins by normalized cell size (SSC-A / median SSC-A), and the mean values for of oxidized (green) to non-oxidized (red) BODIPY-C11 ratio were plotted for each bin (black line). Gray shaded area denotes the s.e.m. for each bin, and the blue area denotes the standard deviation. (E) For Era2-treated cell populations, live cells were identified and gated in the indicated region using a live/dead cell permeability dye SYTOX Blue. (F) Size-dependent lipid peroxidation in RPE-1 cells treated with 0.2 μM Era2 for 20 h. The analysis was performed as in panel (D). (G-I) Proteomics-based analysis of GPX4 (G), ferritin heavy chain (H) and ferritin light chain (I) expression in FACS-sorted small, medium and large RPE-1 cells and primary lung fibroblasts (HLF). Each line in the plot corresponds to a unique peptide from the indicated proteins identified by mass spectrometry reported in *Lanz et al.* (Lanz et al, 2022).

between these two parameters (Fig. 3C,D). We then performed a similar analysis on Era2-treated cells. For this analysis, we gated only live cells using a fluorescent cell permeability dye SYTOX Blue that stains dead or dying cells to omit cells undergoing Era2-induced death (Fig. 3E). This gating allowed us to exclusively focus on the live cells that were not dying. We found that in Era2-treated cell populations, larger cells demonstrated lower levels of lipid peroxidation, similarly to untreated cells (Fig. 3F). By contrast, membrane lipid peroxidation, the terminal cause of ferroptosis, exhibits higher basal levels in smaller cells. This provided a rationale for why smaller cells would require less treatment with Era2 to accumulate enough lipid peroxidation and induce ferroptosis.

Having determined that membrane lipid peroxidation decreases with cell size, we next investigated how the expression of key cellular components regulating this process changes with cell size. The overall lipid oxidation status in the membrane is set largely by the competition between Fe^{2+}-dependent peroxidation of PUFA-containing phospholipids, and glutathione-dependent reduction of peroxidized lipids by GPX4 (Fig. 3A). We analyzed size-dependent proteomics data for RPE-1 cells and primary human lung fibroblasts (HLF) and observed no significant size-differences in GPX4 expression (Fig. 3G). However, ferritin heavy chain (FTH1) and ferritin light chain (FTL) concentrations increased by 1.6-to-2-fold with a two-fold increase in cell size (Fig. 3H,I). Ferritin acts as a key iron-storage protein that can promote ferroptosis resistance through iron chelation (Zhang et al, 2022a; Chen et al, 2020a). The observed increase in ferritin concentration with cell size could therefore lead to additional Fe^{2+} ion chelation, which in turn would protect large cells from iron-dependent lipid peroxidation and ferroptosis. However, when we measured the concentration of labile intracellular Fe^{2+} using a fluorescent probe FerroOrange (Hirayama et al, 2020), we did not observe any size-dependent decrease in labile iron concentration (Fig. S2A). Previous work suggests a link between increased sequestration of ferrous iron in lysosomes and resistance to ferroptosis. It was reported that senescent cells, which are also large (Fig. S3A,B), gain resistance to ferroptosis through lysosomal alkalinization and sequestration of ferrous iron in lysosomes (Loo et al, 2025). We therefore tested whether the superscaling of lysosomes observed in large cells (Lanz et al, 2022; You et al, 2025) promotes Era2 resistance through lysosomal iron sequestration. To do this, we stained the cells with the lysosomal iron detection probe Lyso-FerroRed (Saimoto et al, 2025) and measured its scaling using flow cytometry (Fig. S2B). We observed that the amount of Lyso-FerroRed, and therefore, the amount of lysosomal iron, scaled in direct proportion to cell size, just like the total cellular protein content (Fig. S2B). These results indicate that iron chelation by ferritin and its sequestration in lysosomes are unlikely to play a crucial role in size-dependent decrease in Era2 sensitivity.

Larger cells have higher concentrations of glutathione

Having shown that lipid peroxidation decreases with cell size and that such a decrease is unlikely to be mediated by changes in labile Fe^{2+} concentration, we next sought to test if cell size also affects glutathione (GSH) abundance, which contributes to oxidized lipid reduction and ferroptosis resistance, and is depleted in cells upon system x_c^- inhibition (but not GPX4 inhibition) (Jiang et al, 2021; Dixon & Olzmann, 2024; Dixon et al, 2012) (Fig. 3A). To determine how cell size affects glutathione synthesis, we re-analyzed our previously collected proteomics data, where we compared the proteomes of FACS-sorted small, medium, and large RPE-1 cells (Lanz et al, 2022) (Fig. 3). We found that concentrations of two key proteins involved in GSH biosynthesis, glutamate-cysteine ligase modifier subunit (GCLM) and glutathione synthetase (GSS), increase with cell size. This indicates that larger cells might have higher GSH production rates (Fig. 4A).

While the upregulation of GSH biosynthesis may promote the resistance of larger cells to ferroptosis, such an upregulation alone cannot explain why larger cells become more resistant to ferroptosis induced by the cystine import inhibitor Era2, but not, for example, by the GPX4 inhibitor RSL3 (Chan et al, 2025) (Figs. 2B, S1B). We found previously that upon mTORC1 inhibition cells can evade cystine deprivation-induced ferroptosis by uptake and catabolism of cysteine-rich extracellular proteins, mostly albumin (Armenta et al, 2022) (Fig. S3C). This

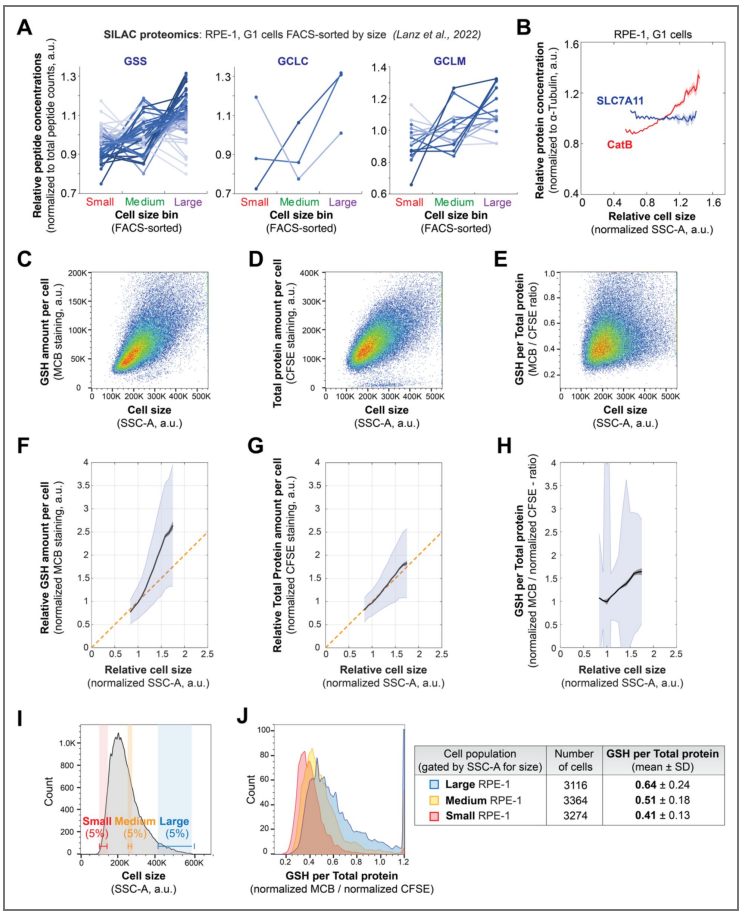

Figure 4. Larger cells have higher concentrations of glutathione and enzymes promoting glutathione synthesis.

(A) Proteomics-based analysis indicates the concentrations of key enzymes involved in glutathione production (see Fig. 3A) increase with cell size. For this analysis, RPE-1 cells were FACS-sorted into populations of small, medium, and large G1 cells, and the proteomes of cells in these bins were analyzed using SILAC mass spectrometry. The primary proteomics data used to plot the concentrations of glutathione synthetase (GSS), glutamate-cysteine ligase catalytic (GCLC) and modifier (GCLM) subunits were taken from our previous work (Lanz et al, 2022). Each line in the plot corresponds to a unique peptide corresponding to the indicated protein that was identified by mass spectrometry. (B) Flow-cytometry-based measurement of cystine/glutamate transporter SLC7A11 (xCT) and cathepsin B (CatB) concentrations in G1-phase RPE-1 cells demonstrates a modest decrease in SLC7A11 and a significant increase in cathepsin B concentrations with cell size. To calculate the concentrations of SLC7A11 and CatB, their amounts were measured with flow cytometry using immunofluorescence and normalized to the amounts of α-Tubulin. The data were binned by cell size, and mean values for each bin were plotted against normalized cell size (solid blue line for SLC7A11 and red line for CatB). Shaded areas denote the s.e.m. for each bin. (C, D) Flow-cytometry-based measurement of GSH amount (C) and total protein amount (D) scaling with cell size in RPE-1 cells. The side scatter parameter (SSC-A) is used as a proxy for cell size (Tzur et al, 2011; Berenson et al, 2019). Three biological replicates were performed, and 100,000 events were recorded in each replicate. (E) GSH concentration in RPE-1 cells plotted against cell size. The GSH concentration is calculated as the ratio of GSH amount to the amount of total protein from data shown in panels (C) and (D). (F-H) Analysis of the flow cytometry data shown in panels (C-E). The data were binned by cell size, and mean values (black lines in the plots) for GSH amount (F), total protein amount (G) and GSH concentration (H) were plotted against normalized cell size (SSC-A / median SSC-A). Gray shaded areas denote the s.e.m. for each bin, and the blue area denotes the standard deviation. The orange line in (F) and (G) is shown for reference and corresponds to a perfect scaling scenario, where the amount of a cell component increases in direct proportion to cell size so that its concentration does not change. The total amount of protein is very close to perfect scaling, while the amount of GSH increases faster than cell size so that its concentration is higher in larger cells. (I, J) Comparison of GSH concentrations in small, medium, and large cells. Based on the flow cytometry data, 5% smallest, 5% largest and 5% intermediate-sized RPE-1 cells were gated (I), and their GSH concentration (GSH amount per total protein amount) histograms were plotted for each of these size populations (J). The plot shows that the GSH concentration distributions progressively shift towards higher values when cell size increases. The plots in (I-J) are based on the primary data shown in panels (C-D).

process involves albumin degradation in lysosomes, predominantly by cathepsin B (CatB), and subsequent export of cystine from lysosomes to fuel the synthesis of glutathione. Large cells undergo proteome rearrangements similar to those occurring upon mTORC1 inhibition (Zatulovskiy et al, 2022). This suggests that large cells may upregulate CatB expression to bypass the Era2-induced cystine import inhibition via system x_c^-. To test this hypothesis, we used flow cytometry to measure how the expression of cathepsin B and the system x_c^- cystine/glutamate transporter SLC7A11 (xCT) scales with cell size (Fig. 4B). We found that SLC7A11 concentration modestly decreases, while CatB concentration significantly increases with cell size (Fig. 4B). This shift in the ratio between SLC7A11 and CatB supports the hypothesis that larger cells may rely less on cystine import via system x_c^- and thus become more resistant to system x_c^- inhibition by Era2.

To further test the prediction that larger cells have more GSH to protect against ferroptosis, we measured GSH abundance in different-sized cells using flow cytometry. To do this, we stained the cells with the fluorescent GSH probe monochlorobimane (MCB) (Rice et al, 1986; Shrieve et al, 1988). In addition to MCB, we also stained the same cells with the total protein dye CFSE (carboxyfluorescein diacetate succinimidyl ester) (Lanz et al, 2022; Berenson et al, 2019), which allowed us to calculate relative cell size-dependent changes in glutathione concentrations (amounts of glutathione per unit protein mass; Fig. 4C-H). While total protein amounts scaled in proportion to cell size (Fig. 4G), the amount of MCB-reactive GSH 'super-scaled' so that larger cells have higher glutathione concentrations than smaller cells (Fig. 4F,H-J). Overall, these findings indicate that larger cells have higher concentrations of glutathione, likely due to their higher concentrations of GSH producing enzymes and cathepsin B, which could specifically protect them from system x_c^- inhibition-induced ferroptosis.

Higher concentrations of ACSL4 in smaller cells drives increased membrane lipid peroxidation

Besides the increase in GSH-producing enzyme concentrations with cell size, our proteomics data also indicate that the concentration of another key protein involved in ferroptosis, Acyl-CoA Synthetase Long Chain Family Member 4 (ACSL4), also changed significantly with cell size (Fig. 4A). ACSL4 promotes ferroptosis sensitivity by enriching phospholipid and triacylglycerol pools with ω-6 PUFAs that are prone to peroxidation (Doll et al, 2017) (Fig. 3A). Our proteomics data (Lanz et al, 2022) suggested that ACSL4 concentration decreases with cell size (Fig. 5A). To confirm this finding using flow cytometry, we stained the cells with antibodies against ACSL4. We observed that the ACSL4 concentration indeed decreases with cell size, while the concentration of the control protein β-actin remains constant (Fig. 5B). This suggested the lower lipid peroxidation in larger calls may be due in part to lower ACSL4 abundance.

To test the role of ACSL4 in size-dependent lipid peroxidation, we measured lipid peroxidation in wild-type and *ACSL4* gene-disrupted HT-1080 cells (Magtanong et al, 2019). We stained the cells with BODIPY-C11 and measured fluorescence with flow cytometry. While lipid peroxidation decreased with increasing cell size in wild-type HT-1080 cells, we did not observe any such size-dependence in *ACSL4 KO* cells (Magtanong et al, 2019) (Fig. 5C,D). This indicated that ACSL4 activity was required for size-dependent changes in basal lipid peroxidation, which likely makes smaller cells more susceptible to ferroptosis.

To test the hypothesis that size-dependent expression of ACSL4 mediates the increased resistance of larger cells to ferroptosis, we FACS-sorted *ACSL4 KO* HMEC cells into small, medium and large size bins and assessed their responses to Era2 (Figs. 5E,F and S4). In this experiment, we synchronized cells in G1 phase using palbociclib prior to cell sorting and also incubated the sorted cells in the presence of palbociclib during Era2 treatment to isolate cell size effects from the previously observed confounding effects of the cell cycle on ferroptosis (Fig. 2B,E). Consistent with our hypothesis, genetic disruption of *ACSL4* reduced the size dependence of the ferroptotic response in Era2-treated HMEC cells (Fig. 5F). We note that while genetic disruption of *ACSL4* significantly reduced the size dependence of ferroptosis, it does not eliminate the size-dependence

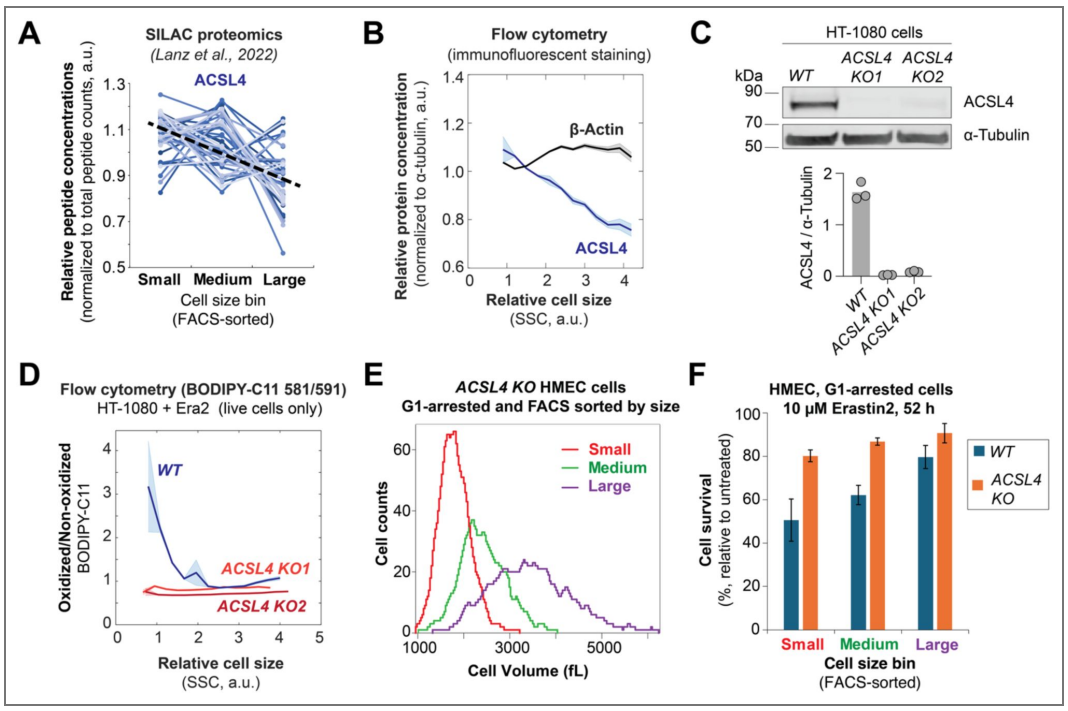

Figure 5. Higher expression of ACSL4 in smaller cells drives increased lipid peroxidation and ferroptosis.

(A) Proteomics analysis identified the size-dependent expression of ACSL4, an enzyme that enriches cellular membranes with long polyunsaturated fatty acids prone to peroxidation (Doll et al, 2017). The primary proteomics data were from our previous work (Lanz et al, 2022). Each line in the plot corresponds to a unique peptide from the ACSL4 protein identified by mass spectrometry; the dashed black line indicated the average ACSL4 protein slope. (B) Flow cytometry analysis confirms the decrease of ACSL4 concentration with cell size in HMEC cells. β-Actin was measured as a reference protein, as its concentration does not change with cell size. To calculate the concentrations of ACSL4 and β-Actin, their amounts were measured with flow cytometry using immunofluorescence and were normalized to the amounts of α-Tubulin. The data were binned by cell size, and mean values for each bin were plotted against normalized cell size (solid blue line for ACSL4 and black line for β-Actin). Shaded areas denote the s.e.m. for each bin. (C) Validation of *ACSL4* knockout in HT-1080 cells with immunoblotting. Wild-type (*WT*) HT-1080 cell line and two different *ACSL4* knockout clones (*KO1* and *KO2*) were analyzed using antibodies against ACSL4 and α-Tubulin as a loading control. Bar plot shows the quantification of immunoblotting data from three biological replicates. (D) Deletion of *ACSL4* eliminates the size-dependence of membrane lipid peroxidation in HT-1080 cells. The plot shows the flow cytometry measurements of lipid peroxidation after 16 h 1 μM Era2 treatment in wild-type and *ACSL4 KO* HT-1080 cells (*ACSL4 KO1* and *ACSL4 KO2* are two different knock-out clones) (Magtanong et al, 2019). The ratio between oxidized (green) BODIPY-C11 and non-oxidized (red) BODIPY-C11 fluorescence is plotted as a metric for lipid peroxidation, and the side-scatter parameter (SSC-A) is used as a proxy for cell size. The flow cytometry data were binned by cell size, and mean values of oxidized to non-oxidized BODIPY-C11 ratios were plotted for each bin (blue solid line corresponds to *wild-type* cells, orange and red lines correspond to *ACSL4* gene-disrupted clones *KO1* and *KO2*). Shaded areas denote the s.e.m. for each bin. (E) Cell size distributions of small, medium, and large G1-arrested *ASCL4 KO* HMEC cells isolated by FACS sorting. Prior to FACS sorting, the cells were cultured for 24 h in the presence of 1 μM palbociclib to synchronize cells in G1 phase. Cell size after sorting was measured on a Coulter counter. (F) Cell survival percentage in *WT* and *ACSL4 KO* HMEC cells, sorted into small, medium, and large size bins by FACS. After sorting, the cells were re-plated in the presence of 1 μM palbociclib to keep them in G1 phase. Cells were then treated with 10 μM Era2 for 52 h, and the cell survival percentage was calculated relative to palbociclib-only treated cells. Cell survival percentages in graphs are shown as means ± s.e.m. for n = 3 biological replicates.

completely. This might be because ferroptosis is driven by two parallel processes – ACSL4-dependent PUFA incorporation into the membrane and subsequent lipid peroxidation (Fig. 3), both of which depend on cell size.

Discussion

In this study, we found that larger cells are less susceptible to ferroptotic cell death induced by the system x_c^- inhibitor erastin2 (Fig. 6). This observation may explain previous findings where genetic alterations that reduce cell size also promote ferroptosis, whereas those that increase cell size inhibit it. For instance, deletion of p21, which decreases cell size, sensitizes to ferroptosis, whereas overexpression of p21, increasing cell size, confers ferroptosis resistance (Tarangelo et al, 2018; Venkatesh et al, 2020). Similarly, deletion of the retinoblastoma protein (RB), which also reduces cell size, promotes ferroptosis. Moreover, further deletion of additional RB family members, p107 and p130, in a triple knockout that drastically reduces cell size, increases sensitivity to ferroptosis (Kuganesan et al, 2021; Sage et al, 2000). Here, we demonstrate that isogenic cell populations differing only in size exhibit different susceptibilities to ferroptosis. This implies that many genetic interactions associated with ferroptosis may actually operate indirectly through their effects on cell size.

That increased cell size protects against system x_c^- inhibitor-induced ferroptosis has important implications for how this form of cell death interacts with the cell division cycle. Cells in G1 phase of the cell cycle were reported to be more susceptible to ferroptosis (Rodencal et al, 2024; Kuganesan et al, 2023), which suggested that ferroptosis inducers could be used in combination with cancer drugs, like the CDK4/6 inhibitor palbociclib, that arrest cells in G1 phase of the cell cycle (Herrera-Abreu et al, 2024). However, while CDK4/6 inhibitors arrest cells in G1, they do not inhibit cell growth, such that the longer they are arrested, the larger the cells grow (Lanz et al, 2022; Crozier et al, 2023; Manohar et al, 2023). This results in a complex, non-monotonic ferroptotic response dynamics in cells treated with CDK4/6 inhibitors (Fig. 2B,E). Just following CDK4/6 inhibitor treatment, as more and more cells are arrested in G1 phase, cells become more sensitive to both RSL3- and erastin-induced ferroptosis (Kuganesan et al, 2023; Rodencal et al, 2024). However, the longer the cells are arrested, the larger they become, which further promotes their susceptibility to RSL3 (Fig. S1B) but reduces their susceptibility to Era2-induced ferroptosis (Fig. 2B). The fact that the cell cycle arrest and cell size increase have opposing effects on Era2-induced ferroptosis susceptibility could explain why different studies reported seemingly contradictory results, where sometimes an increased and sometimes a decreased or unchanged sensitivity to system x_c^- inhibitors was observed depending on the cell type, duration and type of cell cycle arrest (Lee et al, 2024; Kuganesan et al, 2023; Rodencal et al, 2024). Such complex interplay between the cell cycle and cell size effects on ferroptosis suggests that combination therapies utilizing CDK4/6 inhibitors and ferroptosis inducers would have to carefully choose a dosage schedule. Additionally, our data suggest that previously reported resistance of senescent cells to ferroptosis can at least partially be due to the increased cell size, a well-established hallmark of senescence (Davies et al, 2022).

That small cells are more prone to ferroptosis is likely related to their proteome and metabolome composition differing from that of larger cells. Here, we found that larger cells both generate fewer peroxidized membrane lipids and accumulate more glutathione, which can be used to reduce and thus detoxify the peroxidized lipids (Fig. 6). Likely, these size-dependent changes in lipid oxidation and glutathione abundance are due to differential cell-size-scaling of different metabolic enzymes in the cell. Larger cells also have higher concentrations of iron-chelating protein ferritin and glutathione-producing enzymes GSS and GCLM that protect cells against ferroptosis, and have lower concentrations of the enzyme ACSL4, which promotes ferroptosis. Indeed, the genetic disruption of *ACSL4* greatly reduced the size-dependence of membrane lipid peroxidation, a ferroptosis trigger, and makes ferroptosis less size-dependent. Taken together, these observations indicate that the size-dependent remodeling of the proteome underlies much of the size-dependent sensitivity to ferroptosis.

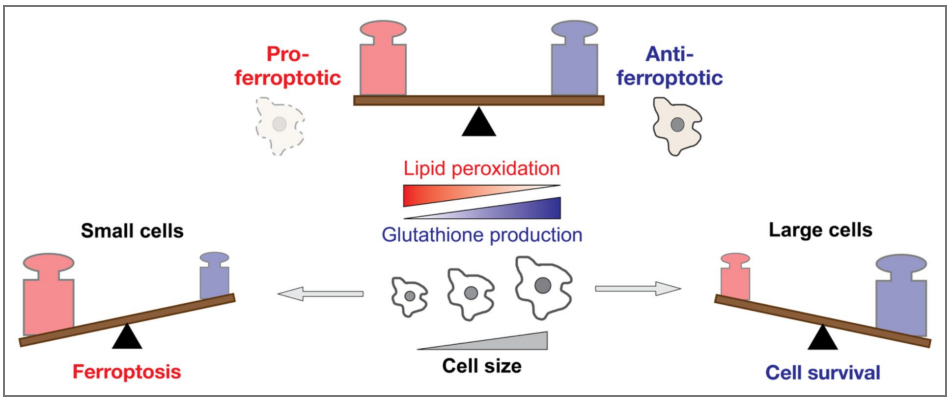

Figure 6. **Cell size modulates cell susceptibility to ferroptosis.**

Larger cells are less prone to Era2-induced cell death because they generate less peroxidized plasma membrane lipids and more glutathione to reduce those toxic peroxidized lipids.

The fact that larger cell size promotes increased ferroptosis resistance to system x_c^- inhibitors (Era2) but, at the same time, decreased resistance to ferroptosis induced by GPX4 inhibitors (RSL3) suggests that the critical roles in these two types of responses are played by different molecular pathways. This finding supports the notion that the ferroptotic cell death response is highly context-dependent and varies dramatically depending on the cell type and class of stimuli inducing ferroptosis (Rodencal et al, 2024; Magtanong et al, 2022; Soula et al, 2020). While a decreased cell sensitivity to Era2 in larger cells is due to size-dependent increase in glutathione production and decrease in unsaturated lipid incorporation into the membrane by ACSL4, the increased sensitivity to RSL3 is reported to be mediated mainly by ER expansion, iron accumulation, and lipid accumulation and remodeling (Chan et al, 2025). We show that large cells may become resistant specifically to Era2 but not RSL3 through the upregulation of lysosomal function, particularly cathepsin B expression, which enables the uptake and catabolism of cysteine-rich extracellular proteins. A size-dependent shift in the ratio between SLC7A11 and cathepsin B makes large cells less dependent on cystine import via system x_c^-, and thus, more resistant to Era2. In addition to this, it was reported that RSL3 can induce ferroptosis independently of GPX4 and may target other selenoproteins (DeAngelo et al, 2025; Cheff et al, 2023), which could also contribute to the difference in size-dependent responses to RSL3 and Era2.

In conclusion, our finding that the response of cells to ferroptosis inducers is influenced by cell size point to a broader pattern where cellular decisions are often size-dependent. A general size-dependence of cellular decisions may be driven by widespread changes in protein and metabolite composition taking place as cells grow larger. Indeed, larger cells differ markedly from their smaller counterparts, which likely affects key decisions related to cell death, division, and differentiation. Previous studies, including our own, have explored how cell size influences cell division and contributes to cellular senescence (Lanz et al, 2022; Zatulovskiy et al, 2022; Crozier et al, 2023, 2022; Manohar et al, 2023; Foy et al, 2023; Wilson et al, 2023; Demidenko & Blagosklonny, 2008). Here, we have demonstrated that cell size also plays a significant role in modulating susceptibility specifically to ferroptotic cell death. Furthermore, research in developmental biology shows that cell size can dictate developmental outcomes, as seen in the asymmetrical division of neurosecretory motor neuron neuroblasts in *C. elegans* and cell fate determination in *Arabidopsis* leaves (Sethi et al, 2022; Gong et al, 2023). Thus, we anticipate many cellular decisions will be impacted by cell size, the fundamental mode of cell geometry that sets the basic scale of all intracellular processes.

Materials and methods

Cell culture conditions and cell lines

Non-transformed *hTERT*-immortalized human mammary epithelium cells (HMEC-*hTERT* cells, in this paper referred to simply as HMEC for brevity) were obtained from Stephen Elledge's laboratory at Harvard Medical School (Solimini et al, 2012) and cultured in MEGM™ Mammary Epithelial Cell Growth Medium (Lonza CC-3150). HT-1080 cells were purchased from ATCC (Manassas, Virginia, USA). Non-transformed *hTERT*-immortalized human retinal pigment epithelium cells (cell line RPE-1) were obtained from the Stearns laboratory at Stanford. Both the HT-1080 and RPE-1 cell lines were grown in Dulbecco's modification of Eagle's medium (DMEM) with L-glutamine, 4.5 g/L glucose and sodium pyruvate (Corning), supplemented with 10% FBS (Corning) and 1% penicillin/streptomycin. All cells were cultured at 37°C with 5% CO_2. HT-1080 cell lines expressing nuclear-localized fluorescent protein mKate2 (Nuc::mKate2) were generated by lentiviral transduction of a viral vector at an M.O.I. of 0.3, that directed the expression of nuclear-localized mKate2 (Forcina et al, 2017). Polyclonal mKate2-expressing populations were selected using puromycin (1.5 mg/mL, 72 h). *ACSL4 KO* HT-1080 and HMEC cells were generated using a CRISPR/Cas9 system, as described previously (Magtanong et al, 2019). RPE-1 cells carrying a genetic construct for a conditional knock-down of cyclin D1 gene (*CCND1)* through doxycycline-inducible *CCND1* shRNA expression were obtained from the Ioannis Sanidas laboratory at Harvard Medical School.

Immunofluorescence cell staining for flow cytometry

For flow cytometry analysis, cells were grown on dishes to ~50% confluence and harvested by trypsinization. The cells were then fixed with 3% formaldehyde for 10 min at 37°C and permeabilized with 90% methanol for 30 min on ice. Fixed and permeabilized cells were washed once with PBS, blocked with 3% BSA in PBS for 30 min at 37°C, and then stained with primary antibodies for 2 h at 37°C (rat-anti-alpha-Tubulin (Abcam, #ab6160), mouse-anti-Actin (Sigma-Aldrich, #A2103), rabbit-anti-ACSL4 (Proteintech, #22401-1-AP), rabbit-anti-Cathepsin B (Proteintech, #12216-1-AP), rabbit-anti-xCT/SLC7A11 (Cell Signaling Technology, #12691T)). The cells were then washed twice with a wash buffer (1% BSA in PBS + 0.05% Tween® 20), stained with the fluorophore-conjugated secondary antibodies Alexa Fluor 488 goat anti-rat (Life Technologies, #A11006), Alexa Fluor 594 goat anti-rabbit (Life Technologies, #A11037), and Alexa Fluor 647 goat anti-mouse (Thermo Fisher Scientific, #A32728) at 1:1000 dilution for 1 h at 37°C. The cells were then washed again twice. After this treatment, the cells were resuspended in PBS containing 3 μM DAPI for DNA staining, incubated for 10 min at room temperature, and then analyzed on an Attune NxT flow cytometer (Thermo Fisher Scientific). Around 100.000 cells were typically recorded for each sample, and three biological replicates were performed for each experiment. The flow cytometry gating strategy is shown in Fig. S5. Briefly, single cells were gated based on FSC-A vs SSC-A, then FSC-A vs FSC-H, then SSC-A vs SSC-W plots. From this population of single cells, G1 cells were selected using Hoechst-A vs FSC-A plot (Fig. S5).

For plotting, all protein amounts and cell size values were normalized to the means for each sample. To compensate for the nonspecific background staining of cells with antibodies, we measured the fluorescence of cells stained with nonspecific Isotype Control antibodies. We then performed a linear regression of this nonspecific background signal with cell size and subtracted the background fluorescence corresponding to each cell's size from the actual anti-ACSL4 fluorescence signal measured for each cell. For all binned flow cytometry data plots, the cells below the 2nd and above the 98th cell size percentiles were excluded to remove the extreme outliers. Then, the remaining data were binned by size and plotted as background-corrected average fluorescence intensity for each bin against the bin's average cell size. Bins with fewer than 200 cells were excluded from the analysis to reduce noise. For protein concentration calculation, the amount of the indicated protein in the cell was normalized to the amount housekeeping protein alpha-Tubulin, which scales in proportion to cell volume (Lanz et al, 2022).

Lipid peroxidation measurement with BODIPY-C11 581/591 fluorescent dye

For lipid peroxidation analysis, cells were treated with DMSO or erastin2 (Era2) for 24 h before being harvested by trypsinization. A cell suspension containing ~200,000 cells was then transferred to a 1.5 mL microfuge tube. Cells were then pelleted by centrifugation (400 x *g*, 5 min) and resuspended in BODIPY-C11 581/591 (5 μM) dissolved in HBSS. A dead cell stain SYTOX Blue (Molecular Probes, #S34857) was added to cell suspensions at a final concentration of 20 nM to identify and exclude from the analysis all non-intact (dead or dying) cells. Cell suspensions were incubated at 37°C for 20 min and then pelleted (400 x *g*, 5 min) and resuspended in 0.2 mL of PBS buffer. Samples were strained through a cell strainer prior to flow cytometry analysis. Flow cytometry analysis was performed on an Attune NxT flow cytometer (Thermo Fisher Scientific). Oxidation of BODIPY-C11 581/591 was calculated as the ratio of the green fluorescence (BL1 channel, indicates oxidized probe) to the red fluorescence (YL1 channel, indicates unoxidized probe) (Dixon et al, 2012; Pap et al, 1999).

Single-cell glutathione (GSH) measurements with MCB fluorescent dye

To measure the GSH amounts in different-sized cells using flow cytometry, we stained the cells with the fluorescent GSH probe monochlorobimane (MCB) (Rice et al, 1986; Shrieve et al, 1988). To do this, the cells were harvested by trypsinization, resuspended in PBS at a density of

one million cells per mL, and incubated with 40 μM MCB (Invitrogen, #M1381MP). At the same time, we stained with MCB, we also stained the same cells with a total protein dye CFSE (CarboxyFluorescein Succinimidyl Ester). For total protein staining, the CellTrace CFSE dye (Molecular Probes, #C34554) was added to cell suspensions at a 5 μM concentration. The cells were then stained with MCB and CFSE for 20 min in a tissue culture incubator (37°C, 5% CO_2) in the dark. The reactions were terminated using 1 mL cold complete medium, followed by centrifugation (400 x *g*, 5 min, +4°C). The pelleted cells were then re-suspended in 0.2 mL of PBS, filtered through a 40 μm cell strainer into FACS tubes and placed on ice. The MCB and CFSE fluorescence signals were measured with an Attune NxT flow cytometer (Thermo Fisher Scientific). GSH concentrations (amounts of glutathione per unit protein mass) in individual cells were calculated as a ratio between the MCB signal (glutathione amount) and CFSE signal (total protein amount).

Intracellular iron detection with fluorescent probes

To measure labile intracellular iron (Fe^{2+}) concentration, live RPE-1 cells were stained simultaneously with three fluorescent probes - FerroOrange (Dojindo Laboratories, Japan, # F374-10) to measure the amounts of labile Fe^{2+} in the cell, CellTrace CFSE dye (Molecular Probes, #C34554) to measure total cellular protein amount, and Hoechst 33342 DNA stain (Thermo Scientific, #62249) to determine the cell cycle phase of the cells. Prior to staining, the cells on a dish were washed twice with warm (37°C) serum-free DMEM and harvested by trypsinization, followed by centrifugation and supernatant removal. The cell pellets were then resuspended in a staining solution containing 1 μM FerroOrange, 5 μM CFSE and 20 μM Hoechst in warm serum-free DMEM and incubated at 37°C for 30 min in a 5% CO2 incubator. After the staining the cells were kept on ice and measured on an Attune NxT flow cytometer (Thermo Fisher Scientific). Hoechst signal was used to select G1-phase cells for subsequent analysis.

A similar protocol was used to measure lysosomal Fe^{2+} amounts, but instead of FerroOrange the cells were stained with 1 μM Lyso-FerroRed probe (Dojindo Laboratories, Japan, # L270-10). After Lyso-FerroRed staining, the cells were centrifuged and washed twice with serum-free DMEM prior to the flow cytometry measurement.

Fluorescence-activated cell sorting (FACS)

Fluorescence-activated cell sorting was used to sort live cells by their size and cell cycle phase, as described previously (Lanz et al, 2022). Cells were harvested from dishes by trypsinization, stained with 20 μM Hoechst 33342 DNA dye in PBS for 15 min at 37°C, and then sorted on a BD FACSAria Fusion flow cytometer. Consecutive SSC-A over FSC-A, and FSC-H over FSC-A gates were used to isolate single cells. Then, G1 cells were gated by DNA content (Hoechst staining). Finally, we collected the 10% smallest and 10% largest cells using the gating based on SSC-A signal as a proxy for cell size. During sorting, all cell samples and collection tubes were kept at 4°C. To determine the cell size distributions of the collected samples, aliquots were taken from each sorted size bin and measured on a Z2 Coulter counter (Beckman). Sorted cells were re-plated for subsequent evaluation of their sensitivity to cell-death-inducing chemicals.

Microscopy-based analysis of cell death kinetics

For the analysis of cell death susceptibility, FACS-sorted small and large G1-phase cells were seeded on a 384-well plate (100-1500 cells per well), allowed to adhere overnight, and then treated with cell-death-inducing compounds for 72 h. Besides these lethal compounds, the cell culture media also contained 20 nM of the dead-cell dye SYTOX Green (Molecular Probes, #S7020), which permeates dying cells and produces a strong green fluorescent signal in cell nuclei. Cells were imaged on the Essen IncuCyte Zoom and analyzed using scalable time-lapse analysis of cell death kinetics (STACK) as described below. Two or three independent biological replicates were performed for each experimental condition. Each of the biological replicates contained two technical replicates for each condition that were then averaged for cell-death sensitivity quantification. Cell death responses were measured using the scalable time-lapse analysis of cell

death kinetics (STACK) technique (Forcina et al, 2017; Inde et al, 2020). Cell lines stably expressing nuclear-localized mKate2 were incubated in medium with 20 nM SYTOX Green and the indicated cell-death-inducing compounds. Counts of live (mKate2+) and dead (SG+) objects were obtained from images acquired every 4 h on the Essen IncuCyte Zoom (Essen BioScience, Ann Arbor, MI). The following image extraction parameter values were used for automated image analysis. For SG+ objects (dead cells): Adaptive Threshold Adjustment 3; Edge Split On; Edge Sensitivity −7; Filter Area min 0 μm^2, max 750 μm^2. For mKate2+ objects (live cells): Adaptive Threshold Adjustment 2.5; Edge Split On; Edge Sensitivity −2; Filter Area min 50 μm^2, maximum 8100 μm^2; Eccentricity max 0.9. For Overlap objects: Filter area min 50 μm^2, maximum 8100 μm^2. Counts were exported to MS Excel (Microsoft Corporation, Redmond, WA) and lethal fraction (LF) scores were computed from mKate2+ and SG+ counts, with the additional step of removing 'overlap' double positive counts from live cell counts at each timepoint, as described before (Forcina et al, 2017; Inde et al, 2020). LF scores were exported to Prism 9.0.1 (GraphPad Software, La Jolla, CA) for curve fitting and data plotting.

Immunoblotting

For immunoblotting, cells were lysed in RIPA lysis buffer on ice. Proteins from lysates were separated on 10% SDS-PAGE gels and transferred to nitrocellulose membranes. Membranes were then blocked with SuperBlock™ (TBS) Blocking Buffer (Thermo Fisher Scientific) and incubated overnight at 4°C with primary antibodies in 3% BSA solution in PBS. The primary antibodies used were: anti-ACSL4 (Sigma-Aldrich, #SAB2701949; 1:2500 dilution) and anti-tubulin (Millipore Sigma, #MS581P1; 1:2000 dilution). The primary antibodies were detected using the fluorescently labeled secondary antibodies IRDye® 680LT Goat anti-Mouse IgG (LI-COR 926-68020) and IRDye® 800CW Goat anti-Rabbit IgG (LI-COR 926-32211). Membranes were imaged on a LI-COR Odyssey CLx and analyzed with LI-COR Image Studio software.

Data quantification, statistical analysis, and software

Lethal fraction calculations and statistical analyses of cell death were performed using Microsoft Excel 14.6.0 (Microsoft Corporation, USA). Flow cytometry data were analyzed using FlowJo 10.6.1 (FlowJo LLC, USA) and Matlab R2022b (MathWorks, USA). Graphing was performed using Prism 9 (GraphPad Software, La Jolla, CA).

Supplementary figures

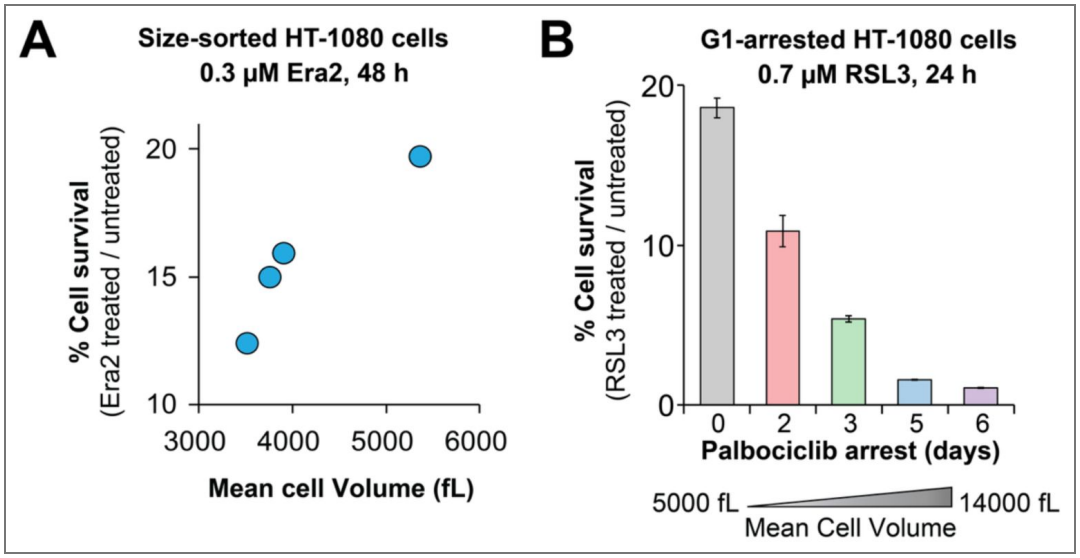

Figure S1. Effects of cell size on Era2- and RSL3-induced ferroptosis susceptibility in HT-1080 cells. (A) Cell survival percentage in HT-1080 cells sorted into four cell size bins using FACS. Cells were treated with 0.3 μM Era2 for 48 h, and cell survival percentage was calculated relative to DMSO-treated cells. The plot shows a

representative example from *n* = 2 biological replicates. Each biological replicate included two technical replicates per condition, which were averaged for quantification of cell size and cell death sensitivity. (B) Cell survival percentage in HT-1080 cells whose size was increased through palbociclib-induced cell cycle arrest. After pre-treatment with palbociclib for the indicated numbers of days, the cells were exposed to 0.7 μM RSL3 in the presence of palbociclib for 24 h. Cell survival percentage was calculated relative to the cells treated only with palbociclib. Cell survival percentages are shown as means ± s.e.m.; n = 3 biological replicates.

Figure S2. Cell size does not affect the concentrations of labile and lysosome-sequestered iron in RPE-1 cells.

(A,B) Flow-cytometry-based measurements of the amount of intracellular labile iron (A) and lysosome-sequestered iron (B) in G1-phase RPE-1 cells. Intracellular labile iron was detected with the FerroOrange fluorescent probe, and lysosomal iron was detected with the Lyso-FerroRed probe. Total cellular protein amount (CFSE staining), which scales in proportion to cell volume, is shown for reference. G1 cells were gated based on Hoechst DNA staining. The data were binned by cell size, and mean values for each bin were plotted against normalized cell size. Shaded areas denote the s.e.m. for each bin. Each sample included 100,000 cells.

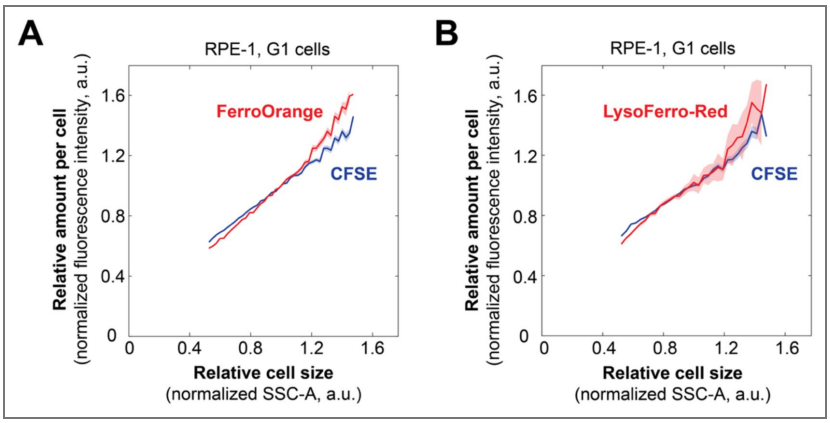

Figure S3. Senescent cells are large and resistant to Era2-induced ferroptosis.

(A) Cell size distributions of senescent and non-senescent (asynchronously proliferating) RPE-1 cells, measured with a Coulter counter. The numbers next to the histograms indicate mean cell size ± standard deviation for each condition. 4-day treatment with 100 nM doxorubicin was used to induce senescence in RPE-1 cells. To reduce the size of senescent cells, 100 nM of the mTORC1 inhibitor rapamycin was added to the media during the 4-day doxorubicin treatment. (B) Cell survival percentage in senescent and non-senescent RPE-1 cells treated with 0.4 μM Era2 for 23 h. Senescent cells demonstrate significantly higher resistance to Era2 than non-senescent cells. Senescent cells pre-treated with rapamycin show only a modest reduction in cell survival. Cell survival percentage was calculated relative to the cells under the same conditions treated with DMSO instead of Era2. Error bars show s.e.m., n = 3 biological replicates. (C) Prolonged cell pre-treatment with 100 nM mTORC1 inhibitor rapamycin causes a moderate decrease in cell sensitivity to Era2.

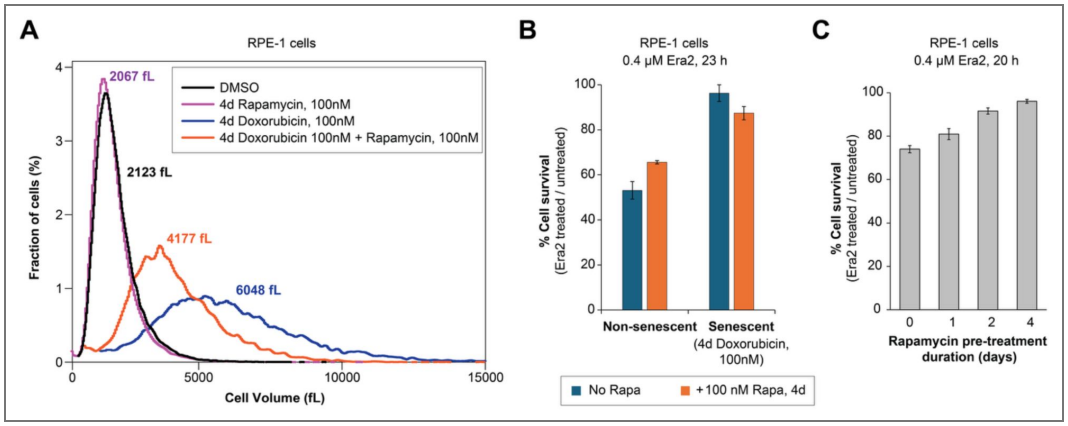

Figure S4. FACS-sorted *ACSL4 KO* HMEC cells have size distributions similar to those of *WT* HMEC cells.

(A) Validation of *ACSL4* knockout in HMEC cells with immunoblotting. Wild-type (*WT*) cell line and a mixed (not clonal) population of *ACSL4* knockout cells were analyzed using antibodies against ACSL4. (B) Mean cell sizes of small, medium, and large *WT* and *ACSL KO* HMEC cells after FACS sorting, measured on a Coulter counter. Error bars indicate cell size S.D. Prior to the sorting, the cells were synchronized in G1 phase by a 24 h treatment with 1 μM palbociclib.

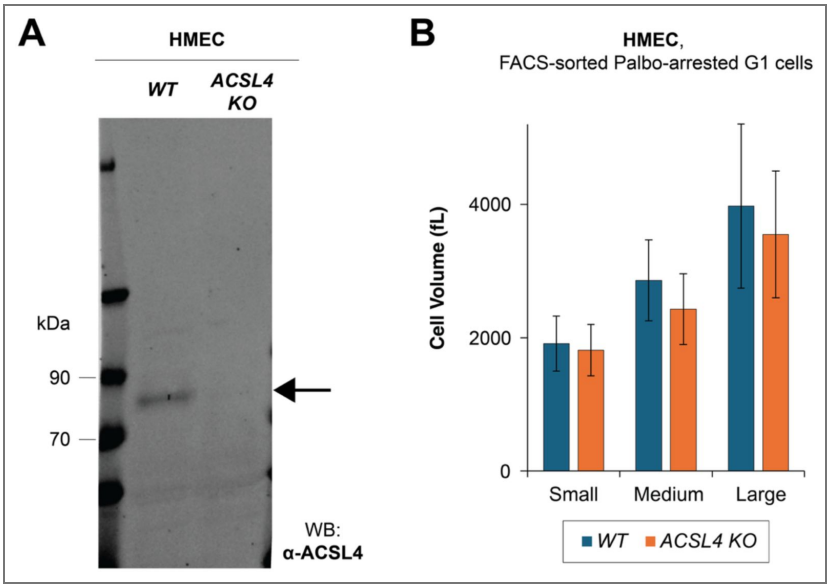

Figure S5. Flow cytometry gating strategy for selecting G1 cells for subsequent scaling analysis.

Single cells were gated based on FSC-A vs SSC-A, then FSC-A vs FSC-H, then SSC-A vs SSC-W plots. From this population of single cells, G1 cells were selected using Hoechst-A vs FSC-A plot for subsequent scaling analysis (the example shown is for cathepsin B scaling analysis).

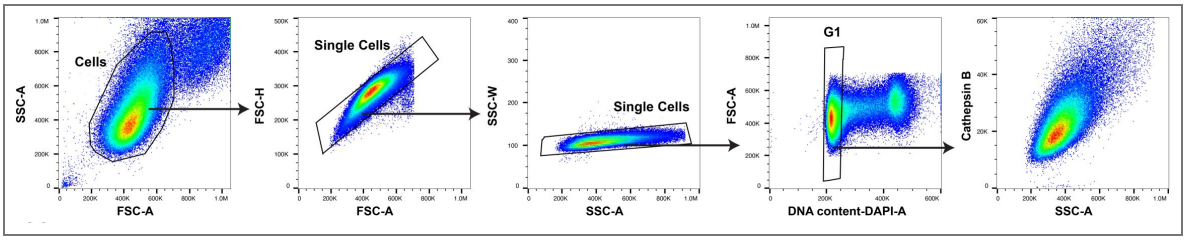

Data availability

All data generated or analyzed during this study are included in the manuscript and supporting files.

Acknowledgements

We thank Leslie Magtanong for assistance with the initial cell death screen design and all members of the Zatulovskiy and Skotheim laboratories for valuable discussions and feedback on this project. Cell sorting for this project was performed on an instrument in the Stanford Shared FACS Facility purchased by Parker Institute for Cancer Immunotherapy, and an instrument in the University of Cambridge, Department of Pathology FACS facility. We thank both FACS facilities for their assistance. This work was supported by a Chan Zuckerberg Biohub Investigator Award (J.M.S.), the NIH (P01 CA254867 grant to J.M.S. and R01 GM122923 to S.J.D.), and the Medical Research Council (MR/X020290/1 Career Development Award to E.Z.).

Additional information

Author contributions

E.Z. conceived this study. E.Z., M.B.M., S.J.D., and J.M.S. designed the experiments. E.Z., M.B.M., and S.Z. performed the experiments and analyzed the experimental data. E.Z. and J.M.S. wrote the manuscript. E.Z., M.B.M., S.J.D., and J.M.S. edited the manuscript.

Funding

Funder	Grant reference number	Author
HHS | NIH | NCI | Center for Cancer Research (CCR)	P01 CA254867	Jan M Skotheim
HHS | NIH | National Institute of General Medical Sciences (NIGMS)	R01 GM122923	Scott J Dixon
UKRI | Medical Research Council (MRC)	MR/X020290/1	Evgeny Zatulovskiy
Chan Zuckerberg Initiative (CZI)	Biohub Investigator Award	Jan M Skotheim

Author ORCID iDs

Evgeny Zatulovskiy: https://orcid.org/0000-0002-7847-5829
Magdalena B Murray: https://orcid.org/0000-0002-6306-4568
Shuyuan Zhang: https://orcid.org/0000-0002-6220-5998
Scott J Dixon: https://orcid.org/0000-0001-6230-8199
Jan M Skotheim: https://orcid.org/0000-0001-8420-6820

References

Armenta DA, Laqtom NN, Alchemy G, Dong W, Morrow D, Poltorack CD, Nathanson DA, Abu-Remaileh M, Dixon SJ (2022) Ferroptosis inhibition by lysosome-dependent catabolism of extracellular protein. *Cell Chemical Biology* **29**:1588-1600. https://doi.org/10.1016/j.chembiol.2022.10.006 | PubMed

Bell CD, Waizbard E (1986) Variability of cell size in primary and metastatic human breast carcinoma. *Invasion Metastasis* **6**:11-20 PubMed

Berenson DF, Zatulovskiy E, Xie S, Skotheim JM (2019) Constitutive expression of a fluorescent protein reports the size of live human cells. *Mol Biol Cell* **30**:2985-2995 https://doi.org/10.1091/mbc.e19-03-0171 | PubMed

Bhatia P, Hachet O, Hersch M, Rincon S, Berthelot-Grosjean M, Dalessi S, Basterra L, Bergmann S, Paoletti A, Martin SG (2014) Distinct levels in Pom1 gradients limit Cdr2 activity and localization to time and position division. *Cell Cycle* **13**:538-552 https://doi.org/10.4161/cc.27411 | PubMed

Chan KY, Yu Y, Kong Y, Cheng L, Yao R, Yin Chair PS, Wang P, Wang R, Sun W-Y, He R-R, *et al.* (2025) GPX4-dependent ferroptosis sensitivity is a fitness trade-of for cell enlargement. *iScience* **28**:112363 https://doi.org/10.1016/j.isci.2025.112363 | PubMed

Chan Y-HM, Marshall WF (2010) Scaling properties of cell and organelle size. *Organogenesis* **6**:88-96 https://doi.org/10.4161/org.6.2.11464 | PubMed

Cheff DM, Huang C, Scholzen KC, Gencheva R, Ronzetti MH, Cheng Q, Hall MD, Arnér ESJ (2023) The ferroptosis inducing compounds RSL3 and ML162 are not direct inhibitors of GPX4 but of TXNRD1. *Redox Biol* **62**:102703 https://doi.org/10.1016/j.redox.2023.102703 | PubMed

Chen C, Inaba M, Venkei ZG, Yamashita YM (2016) Klp10A, a stem cell centrosome-enriched kinesin, balances asymmetries in Drosophila male germline stem cell division. *eLife* **5**:e20977 https://doi.org/10.7554/eLife.20977 | PubMed

Chen X, Yu C, Kang R, Tang D (2020a) Iron Metabolism in Ferroptosis. *Front Cell Dev Biol* 8 https://doi.org/10.3389/fcell.2020.590226 | PubMed

Chen Y, Zhao G, Zahumensky J, Honey S, Futcher B (2020b) Diferential Scaling of Gene Expression with Cell Size May Explain Size Control in Budding Yeast. *Molecular Cell* **78**:359-370. https://doi.org/10.1016/j.molcel.2020.03.012 | PubMed

Conlon I, Raff M (2003) Diferences in the way a mammalian cell and yeast cells coordinate cell growth and cell-cycle progression. *J Biol* **2**:7 https://doi.org/10.1186/1475-4924-2-7 | PubMed

Cordes S, Frank CA, Garriga G (2006) The C. elegans MELK ortholog PIG-1 regulates cell size asymmetry and daughter cell fate in asymmetric neuroblast divisions. *Development* **133**:2747-2756 https://doi.org/10.1242/dev.02447 | PubMed

Crozier L, Foy R, Adib R, Kar A, Holt JA, Pareri AU, Valverde JM, Rivera R, Weston WA, Wilson R, *et al.* (2023) CDK4/6 inhibitor-mediated cell overgrowth triggers osmotic and replication stress to promote senescence. *Mol Cell* **83**:4062-4077. https://doi.org/10.1016/j.molcel.2023.10.016 | PubMed

Crozier L, Foy R, Mouery BL, Whitaker RH, Corno A, Spanos C, Ly T, Gowen Cook J, Saurin AT (2022) CDK4/6 inhibitors induce replication stress to cause long-term cell cycle withdrawal. *EMBO J* **41**:e108599 https://doi.org/10.15252/embj.2021108599 | PubMed

Davies DM, van den Handel K, Bharadwaj S, Lengefeld J (2022) Cellular enlargement - A new hallmark of aging?. *Frontiers in Cell and Developmental Biology* **10** https://doi.org/10.3389/fcell.2022.1036602 | PubMed

DeAngelo SL, Zhao L, Dziechciarz S, Shin M, Solanki S, Balia A, El-Derany MO, Castillo C, Qin Y, Das NK, *et al.* (2025) Recharacterization of the Tumor Suppressive Mechanism of RSL3 Identifies the Selenoproteome as a Druggable Pathway in Colorectal Cancer. *Cancer Res* **85**:2788-2804 https://doi.org/10.1158/0008-5472.can-24-3478 | PubMed

Demidenko ZN, Blagosklonny MV (2008) Growth stimulation leads to cellular senescence when the cell cycle is blocked. *Cell Cycle* **7**:3355-3361 https://doi.org/10.4161/cc.7.21.6919 | PubMed

Dixon SJ, Lemberg KM, Lamprecht MR, Skouta R, Zaitsev EM, Gleason CE, Patel DN, Bauer AJ, Cantley AM, Yang WS, *et al.* (2012) Ferroptosis: An Iron-Dependent Form of Nonapoptotic Cell Death. *Cell* **149**:1060-1072 https://doi.org/10.1016/j.cell.2012.03.042 | PubMed

Dixon SJ, Olzmann JA (2024) The cell biology of ferroptosis. *Nat Rev Mol Cell Biol* 1-19 https://doi.org/10.1038/s41580-024-00703-5 | PubMed

Dixon SJ, Patel DN, Welsch M, Skouta R, Lee ED, Hayano M, Thomas AG, Gleason CE, Tatonetti NP, Slusher BS, *et al.* (2014) Pharmacological inhibition of cystine–glutamate exchange induces endoplasmic reticulum stress and ferroptosis. *eLife* **3**:e02523 https://doi.org/10.7554/eLife.02523 | PubMed

Doll S, Proneth B, Tyurina YY, Panzilius E, Kobayashi S, Ingold I, Irmler M, Beckers J, Aichler M, Walch A, *et al.* (2017) ACSL4 dictates ferroptosis sensitivity by shaping cellular lipid composition. *Nat Chem Biol* **13**:91-98 https://doi.org/10.1038/nchembio.2239 | PubMed

Forcina GC, Conlon M, Wells A, Cao JY, Dixon SJ (2017) Systematic Quantification of Population Cell Death Kinetics in Mammalian Cells. *Cell Syst* **4**:600-610.6 https://doi.org/10.1016/j.cels.2017.05.002 | PubMed

Foy R, Crozier L, Pareri AU, Valverde JM, Park BH, Ly T, Saurin AT (2023) Oncogenic signals prime cancer cells for toxic cell overgrowth during a G1 cell cycle arrest. *Molecular Cell* **83**:4047-4061. https://doi.org/10.1016/j.molcel.2023.10.020 | PubMed

Ginzberg MB, Chang N, D'Souza H, Patel N, Kafri R, Kirschner MW (2018) Cell size sensing in animal cells coordinates anabolic growth rates and cell cycle progression to maintain cell size uniformity. *eLife* **7**:e26957 https://doi.org/10.7554/eLife.26957 | PubMed

Ginzberg MB, Kafri R, Kirschner M (2015) Cell biology. On being the right (cell) size. *Science* **348**:1245075 https://doi.org/10.1126/science.1245075 | PubMed

Gong Y, Dale R, Fung HF, Amador GO, Smit ME, Bergmann DC (2023) A cell size threshold triggers commitment to stomatal fate in Arabidopsis. *Science Advances* **9**:eadf3497 https://doi.org/10.1126/sciadv.adf3497 | PubMed

Hatzold J, Conradt B (2008) Control of Apoptosis by Asymmetric Cell Division. *PLOS Biology* **6**:e84 https://doi.org/10.1371/journal.pbio.0060084 | PubMed

Herrera-Abreu MT, Guan J, Khalid U, Ning J, Costa MR, Chan J, Li Q, Fortin J-P, Wong WR, Perampalam P, *et al.* (2024) Inhibition of GPX4 enhances CDK4/6 inhibitor and endocrine therapy activity in breast cancer. *Nat Commun* **15**:9550 https://doi.org/10.1038/s41467-024-53837-7 | PubMed

Hirayama T, Niwa M, Hirosawa S, Nagasawa H (2020) High-Throughput Screening for the Discovery of Iron Homeostasis Modulators Using an Extremely Sensitive Fluorescent Probe. *ACS Sens* **5**:2950-2958 https://doi.org/10.1021/acssensors.0c01445 | PubMed

Inde Z, Forcina GC, Denton K, Dixon SJ (2020) Kinetic Heterogeneity of Cancer Cell Fractional Killing. *Cell Reports* **32**:107845 https://doi.org/10.1016/j.celrep.2020.107845 | PubMed

Jiang X, Stockwell BR, Conrad M (2021) Ferroptosis: mechanisms, biology and role in disease. *Nat Rev Mol Cell Biol* **22**:266-282 https://doi.org/10.1038/s41580-020-00324-8 | PubMed

Kiyomitsu T, Cheeseman IM (2013) Cortical Dynein and Asymmetric Membrane Elongation Coordinately Position the Spindle in Anaphase. *Cell* **154**:391-402 https://doi.org/10.1016/j.cell.2013.06.010 | PubMed

Kuganesan N, Dlamini S, Tillekeratne LMV, Taylor WR (2021) Tumor suppressor p53 promotes ferroptosis in oxidative stress conditions independent of modulation of ferroptosis by p21, CDKs, RB, and E2F. *J Biol Chem* **297**:101365 https://doi.org/10.1016/j.jbc.2021.101365 | PubMed

Kuganesan N, Dlamini S, Tillekeratne VL, Taylor WR (2023) Regulation of Ferroptosis by Transcription Factor E2F1 and RB. *Research Square* https://doi.org/10.21203/rs.3.rs-2493335/v1

Lanz MC, Zatulovskiy E, Swafer MP, Zhang L, Ilerten I, Zhang S, You DS, Marinov G, McAlpine P, Elias JE, *et al.* (2022) Increasing cell size remodels the proteome and promotes senescence. *Molecular Cell* **82**:3255-3269. https://doi.org/10.1016/j.molcel.2022.07.017 | PubMed

Lanz MC, Zhang S, Swafer MP, Ziv I, Götz LH, Kim J, McCarthy F, Jarosz DF, Elias JE, Skotheim JM (2024) Genome dilution by cell growth drives starvation-like proteome remodeling in mammalian and yeast cells. *Nat Struct Mol Biol* **31**:1859-1871 https://doi.org/10.1038/s41594-024-01353-z | PubMed

Lee H, Horbath A, Kondiparthi L, Meena JK, Lei G, Dasgupta S, Liu X, Zhuang L, Koppula P, Li M, *et al.* (2024) Cell cycle arrest induces lipid droplet formation and confers ferroptosis resistance. *Nat Commun* **15**:79 https://doi.org/10.1038/s41467-023-44412-7 | PubMed

Lengefeld J, Cheng C-W, Maretich P, Blair M, Hagen H, McReynolds MR, Sullivan E, Majors K, Roberts C, Kang JH, *et al.* (2021) Cell size is a determinant of stem cell potential during aging. *Sci Adv* **7**:eabk0271 https://doi.org/10.1126/sciadv.abk0271 | PubMed

Li Q, Rycaj K, Chen X, Tang DG (2015) Cancer stem cells and cell size: A causal link?. *Semin Cancer Biol* **35**:191-199 https://doi.org/10.1016/j.semcancer.2015.07.002 | PubMed

Liao Y-H, Chen S-Y, Chou S-Y, Wang P-H, Tsai M-R, Sun C-K (2012) Determination of chronological aging parameters in epidermal keratinocytes by in vivo harmonic generation microscopy. *Biomed Opt Express* **4**:77-88 https://doi.org/10.1364/boe.4.000077 | PubMed

Liu X, Yan J, Kirschner MW (2024) Cell size homeostasis is tightly controlled throughout the cell cycle. *PLOS Biology* **22**:e3002453 https://doi.org/10.1371/journal.pbio.3002453 | PubMed

Loo TM, Zhou X, Tanaka Y, Sugawara S, Yamauchi S, Kawasaki H, Matsuoka Y, Sugiura Y, Sakuma S, Yamanishi Y, *et al.* (2025) Senescence-associated lysosomal dysfunction impairs cystine deprivation-induced lipid peroxidation and ferroptosis. *Nat Commun* **16**:6617 https://doi.org/10.1038/s41467-025-61894-9 | PubMed

Magtanong L, Ko P-J, To M, Cao JY, Forcina GC, Tarangelo A, Ward CC, Cho KY, Patti GJ, Nomura DK, *et al.* (2019) Exogenous Monounsaturated Fatty Acids Promote a Ferroptosis-Resistant Cell State. *Cell Chem Biol* **26**:420-432.e9 https://doi.org/10.1016/j.chembiol.2018.11.016 | PubMed

Magtanong L, Mueller GD, Williams KJ, Billmann M, Chan K, Armenta DA, Mofat J, Boone C, Myers CL, Olzmann JA, *et al.* (2022) Context-Dependent Regulation of Ferroptosis Sensitivity. *Cell Chem Biol* **29**:1409-1418.e6 https://doi.org/10.1016/j.chembiol.2022.06.004 | PubMed

Manohar S, Estrada ME, Uliana F, Vuina K, Alvarez PM, de Bruin RAM, Neurohr GE (2023) Genome homeostasis defects drive enlarged cells into senescence. *Mol Cell* **83**:4032-4046. https://doi.org/10.1016/j.molcel.2023.10.018 | PubMed

Martin SG, Berthelot-Grosjean M (2009) Polar gradients of the DYRK-family kinase Pom1 couple cell length with the cell cycle. *Nature* **459**:852-856 https://doi.org/10.1038/nature08054 | PubMed

Miettinen TP, Björklund M (2016) Cellular Allometry of Mitochondrial Functionality Establishes the Optimal Cell Size. *Dev Cell* **39**:370-382 https://doi.org/10.1016/j.devcel.2016.09.004 | PubMed

Miller KE, Vargas-Garcia C, Singh A, Moseley JB (2023) The fission yeast cell size control system integrates pathways measuring cell surface area, volume, and time. *Current Biology* **33**:3312-3324. https://doi.org/10.1016/j.cub.2023.06.054 | PubMed

Moseley JB, Nurse P (2010) Cell Division Intersects with Cell Geometry. *Cell* **142**:189-193 https://doi.org/10.1016/j.cell.2010.07.004 | PubMed

Neurohr GE, Terry RL, Lengefeld J, Bonney M, Brittingham GP, Moretto F, Miettinen TP, Vaites LP, Soares LM, Paulo JA, *et al.* (2019) Excessive Cell Growth Causes Cytoplasm Dilution And Contributes to Senescence. *Cell* **176**:1083-1097. https://doi.org/10.1016/j.cell.2019.01.018 | PubMed

Nguyen A, Yoshida M, Goodarzi H, Tavazoie SF (2016) Highly variable cancer subpopulations that exhibit enhanced transcriptome variability and metastatic fitness. *Nat Commun* **7**:11246 https://doi.org/10.1038/ncomms11246 | PubMed

Pan KZ, Saunders TE, Flor-Parra I, Howard M, Chang F (2014) Cortical regulation of cell size by a sizer cdr2p. *eLife* **3**:e02040 https://doi.org/10.7554/eLife.02040 | PubMed

Pap EH, Drummen GP, Winter VJ, Kooij TW, Rijken P, Wirtz KW, Op den Kamp JA, Hage WJ, Post JA (1999) Ratio-fluorescence microscopy of lipid oxidation in living cells using C11-BODIPY(581/591). *FEBS Lett* **453**:278-282 https://doi.org/10.1016/s0014-5793(99)00696-1 | PubMed

Rice GC, Bump EA, Shrieve DC, Lee WL, Kovacs MK (1986) Quantitative Analysis of Cellular Glutathione by Flow Cytometry Utilizing Monochlorobimane: Some Applications to Radiation and Drug Resistance in Vitro and in Vivo. *Cancer Research* **46**:6105-6110 PubMed

Rodencal J, Kim N, He A, Li VL, Lange M, He J, Tarangelo A, Schafer ZT, Olzmann JA, Long JZ, *et al.* (2024) Sensitization of cancer cells to ferroptosis coincident with cell cycle arrest. *Cell Chem Biol* **31**:234-248. https://doi.org/10.1016/j.chembiol.2023.10.011 | PubMed

Ruiz-Losada M, González R, Peropadre A, Gil-Gálvez A, Tena JJ, Baonza A, Estella C (2022) Coordination between cell proliferation and apoptosis after DNA damage in Drosophila. *Cell Death DiEer* **29**:832-845 https://doi.org/10.1038/s41418-021-00898-6 | PubMed

Sage J, Mulligan GJ, Attardi LD, Miller A, Chen S, Williams B, Theodorou E, Jacks T (2000) Targeted disruption of the three Rb-related genes leads to loss of G1 control and immortalization. *Genes Dev* **14**:3037-3050 https://doi.org/10.1101/gad.843200 | PubMed

Saimoto Y, Kusakabe D, Morimoto K, Matsuoka Y, Kozakura E, Kato N, Tsunematsu K, Umeno T, Kiyotani T, Matsumoto S, *et al.* (2025) Lysosomal lipid peroxidation contributes to ferroptosis induction via lysosomal membrane permeabilization. *Nat Commun* **16**:3554 https://doi.org/10.1038/s41467-025-58909-w | PubMed

Sandlin CW, Gu S, Xu J, Deshpande C, Feldman MD, Good MC (2022) Epithelial cell size dysregulation in human lung adenocarcinoma. *PLOS One* **17**:e0274091 https://doi.org/10.1371/journal.pone.0274091 | PubMed

Schmoller KM, Turner JJ, Kõivomägi M, Skotheim JM (2015) Dilution of the cell cycle inhibitor Whi5 controls budding-yeast cell size. *Nature* **526**:268-272 https://doi.org/10.1038/nature14908 | PubMed

Sethi A, Wei H, Mishra N, Segos I, Lambie EJ, Zanin E, Conradt B (2022) A caspase–RhoGEF axis contributes to the cell size threshold for apoptotic death in developing Caenorhabditis elegans. *PLOS Biology* **20**:e3001786 https://doi.org/10.1371/journal.pbio.3001786 | PubMed

Shrieve DC, Bump EA, Rice GC (1988) Heterogeneity of cellular glutathione among cells derived from a murine fibrosarcoma or a human renal cell carcinoma detected by flow cytometric analysis. *Journal of Biological Chemistry* **263**:14107-14114 https://doi.org/10.1016/s0021-9258(18)68191-8 | PubMed

Solimini NL, Xu Q, Mermel CH, Liang AC, Schlabach MR, Luo J, Burrows AE, Anselmo AN, Bredemeyer AL, Li MZ, *et al.* (2012) Recurrent Hemizygous Deletions in Cancers May Optimize Proliferative Potential. *Science* **337**:104-109 https://doi.org/10.1126/science.1219580 | PubMed

Soula M, Weber RA, Zilka O, Alwaseem H, La K, Yen F, Molina H, Garcia-Bermudez J, Pratt DA, Birsoy K (2020) Metabolic determinants of cancer cell sensitivity to canonical ferroptosis inducers. *Nat Chem Biol* **16**:1351-1360 https://doi.org/10.1038/s41589-020-0613-y | PubMed

Tarangelo A, Magtanong L, Bieging-Rolett KT, Li Y, Ye J, Attardi LD, Dixon SJ (2018) p53 Suppresses Metabolic Stress-Induced Ferroptosis in Cancer Cells. *Cell Rep* **22**:569-575 https://doi.org/10.1016/j.celrep.2017.12.077 | PubMed

Tzur A, Moore JK, Jorgensen P, Shapiro HM, Kirschner MW (2011) Optimizing Optical Flow Cytometry for Cell Volume-Based Sorting and Analysis. *PLOS One* **6**:e16053 https://doi.org/10.1371/journal.pone.0016053 | PubMed

Venkatesh D, Stockwell BR, Prives C (2020) p21 can be a barrier to ferroptosis independent of p53. *Aging* **12**:17800-17814 https://doi.org/10.18632/aging.103961 | PubMed

Wilson GA, Vuina K, Sava G, Huard C, Meneguello L, Coulombe-Huntington J, Bertomeu T, Maizels RJ, Lauring J, Kriston-Vizi J, *et al.* (2023) Active growth signaling promotes senescence and cancer cell sensitivity to CDK7 inhibition. *Molecular Cell* **83**:4078-4092. https://doi.org/10.1016/j.molcel.2023.10.017 | PubMed

Yang WS, SriRamaratnam R, Welsch ME, Shimada K, Skouta R, Viswanathan VS, Cheah JH, Clemons PA, Shamji AF, Clish CB, *et al.* (2014) Regulation of Ferroptotic Cancer Cell Death by GPX4. *Cell* **156**:317-331 https://doi.org/10.1016/j.cell.2013.12.010 | PubMed

You DS, Bohrer CH, Rumde PH, Sanidas I, Swafer MP, Larson DR, Elias JE, Lanz MC, Skotheim JM (2025) Cell size-dependent mRNA transcription drives proteome remodeling. *bioRxiv* https://doi.org/10.1101/2025.10.30.685141

Zatulovskiy E, Lanz MC, Zhang S, McCarthy F, Elias JE, Skotheim JM (2022) Delineation of proteome changes driven by cell size and growth rate. *Front Cell Dev Biol* **10**:980721 https://doi.org/10.3389/fcell.2022.980721 | PubMed

Zatulovskiy E, Skotheim JM (2020) On the Molecular Mechanisms Regulating Animal Cell Size Homeostasis. *Trends Genet* **36**:360-372 https://doi.org/10.1016/j.tig.2020.01.011 | PubMed

Zatulovskiy E, Zhang S, Berenson DF, Topacio BR, Skotheim JM (2020) Cell growth dilutes the cell cycle inhibitor Rb to trigger cell division. *Science* **369**:466-471 https://doi.org/10.1126/science.aaz6213 | PubMed

Zhang N, Yu X, Song L, Xiao Z, Xie J, Xu H (2022a) Ferritin confers protection against iron-mediated neurotoxicity and ferroptosis through iron chelating mechanisms in MPP+-induced MES23.5 dopaminergic cells. *Free Radical Biology and Medicine* **193**:751-763 https://doi.org/10.1016/j.freeradbiomed.2022.11.018 | PubMed

Zhang S, Valenzuela LF, Zatulovskiy E, Mangiante L, Curtis C, Skotheim JM (2024) The G1-S transition is promoted by Rb degradation via the E3 ligase UBR5. *Science Advances* https://doi.org/10.1126/sciadv.adq6858 | PubMed

Zhang S, Zatulovskiy E, Arand J, Sage J, Skotheim JM (2022b) The cell cycle inhibitor RB is diluted in G1 and contributes to controlling cell size in the mouse liver. *Frontiers in Cell and Developmental Biology* 10 https://doi.org/10.3389/fcell.2022.965595 | PubMed

Peer reviews

Reviewer #1 (Public review):

Summary:

The study by Zatulovskiy et al. examined how cell size influences cell susceptibility to ferroptosis. The authors found a size dependence specifically for ferroptosis-inducing drug Era2, but not for other drugs. Using various human cell lines (HMEC, HT 1080, RPE 1), the authors generated populations of small and large G1 cells by FACS, CDK4/6 inhibition (palbociclib), or inducible cyclin D1 knockdown, and measured cell susceptibility to ferroptosis. Larger cells were more resistant than smaller cells. Mechanistically, larger cells showed reduced plasma membrane lipid peroxidation, higher glutathione concentrations, and changes in relevant cellular proteins levels, as analyzed using previously published data. Deleting ACSL4, which is involved in ferroptosis, partly eliminated the size dependence of ferroptosis. The work concludes that cell size is a key determinant of ferroptosis susceptibility. Overall, this work expands our understanding of how cell size is correlated with functional properties of cells, which can have implications for biomedical sciences.

Strengths:

The study establishes a credible link between cell size and susceptibility to ferroptosis, as induced by Era2. Experimental replication is sufficient, and key conclusions rely on data from multiple cell lines and on multiple approaches to manipulate cell size. This suggests that the conceptual findings made in this paper could reflect a more fundamental feature of mammalian cells. In addition, this work provides an interesting contrast to another recent study about size-dependency of ferroptosis (*https://doi.org/10.1016/j.isci.2025.112363*), where increased cell size heightened sensitivity to the GPX4 inhibitor RSL3.

Original Weaknesses:

Disentangling cell size effects from other confounding factors, such as the cell cycle or overall metabolic rate, is challenging, and the authors have managed to qualitatively prove that cell size influences Era2-induced ferroptosis. However, the quantitative nature of this link between cell size and susceptibility to ferroptosis remains somewhat unclear due to the confounding factors that are present in many of their experiments. Notably, the quantitative nature of this link could also be cell type and growth condition -dependent, which remain to be investigated in detail. It should also be noted that this work focused on cell culture studies, and it remains unclear how much the findings of this paper could influence therapeutic strategies in vivo.

Comments on revised version:

I would first like to emphasize that I find this work solid, and I think the authors have done good work with the revisions.

My only remaining recommendation is that the authors aim to more carefully examine the magnitude of the observed cell size-dependency in ferroptosis susceptibility. Their manuscript contains several experiments where the quantitative nature of this link remains unclear due to confounding factors, such as the cell cycle. For example, in Fig 2B&C, it seems that accumulation of cells in G1 (from ~60% to ~95%) decreases ferroptosis equally to the effect caused by cell volume doubling (from day 2 to day 4 of palbo treatment), suggesting that cell cycle has a much more pronounced effect on ferroptosis than cell size (especially when considering the size change from day 0 to day 2). However, the magnitude of the cell size effect is not consistent between all experiments shown. This is not surprising, as the authors use different approaches to changing cell size and different cell lines, but it makes the work more qualitative than quantitative. Notably, another confounding factor is the cell's metabolic/biosynthetic rate. It seems reasonable to assume that prolonged palbociclib treatment will decrease metabolic and protein synthesis rates (normalized to cell size), and this could make the cells less susceptible to ferroptosis. The rapamycin treatment results shown by the authors also support this notion. One approach to examining this could be to grow cells in various growth conditions to manipulate their growth & metabolic rate.

https://doi.org/10.7554/eLife.111544.1.sa3

Reviewer #2 (Public review):

Summary:

The authors set out to understand how cell phenotypes differ depending on the size of the cell, specifically here how cell size affects cell death. Using human cell lines (HMEC, HT-1080, RPE-1), the authors examined cell size through FACS sorting, CDK4/6 inhibition and inducible cyclin D1 knockdown. They identify that larger cells are more resistant to ferroptosis induced by system xc^- inhibition (erastin2), but more sensitive to GPX4 inhibition (RSL3), highlighting pathway-specific size dependencies.

Mechanistically, larger cells exhibited:

- Higher glutathione levels, supporting lipid peroxide detoxification

- Increased ferritin expression, promoting iron sequestration

- Lower ACSL4 levels, reducing incorporation of peroxidation-prone lipids

The findings are supported by high-throughput microscopy, flow cytometry (BODIPY-C11 lipid peroxidation assays), and proteomic analyses. The study concludes that cell size influences proteome composition and metabolic capacity, thereby shaping cell death decisions, an insight with implications for aging, cancer, and ferroptosis-based therapies.

Major Strengths:

- use of multiple cell lines to validate their findings

- use of multiple, complimentary approaches

- well designed screen and experiments throughout

- clearly written, logical flow and easy to follow

- relevance for multiple fields

Weaknesses:

- Lack of in-depth mechanistic investigation

- Experiments are all in vitro and so, as yet, it is uncertain what the in vivo consequence would be

General Assessment:

This study presents a mechanistic link between cell size and ferroptosis susceptibility. Using high-throughput microscopy, proteomics, and genetic perturbations across multiple human cell lines, the authors demonstrate that larger cells are more resistant to ferroptosis induced by system xc^- inhibition (erastin2). This resistance is attributed to elevated glutathione production, increased ferritin-mediated iron sequestration, and reduced ACSL4-dependent lipid peroxidation. The experimental design is rigorous and multifaceted, with consistent results across cell types and size manipulation methods. While the study is limited to in vitro systems, its conceptual and mechanistic insights lay the groundwork for future in vivo and translational investigations.

Advance:

This work is the first to systematically show that cell size directly influences ferroptosis susceptibility via proteome scaling. It reconciles previous findings that large cells are sensitized to GPX4 inhibition (RSL3) by demonstrating that the ferroptosis pathway targeted system xc^- vs GPX4 determines the direction of size-dependent vulnerability. The study provides a conceptual advance by positioning cell size as a regulatory axis in cell death decisions, and a mechanistic advance by identifying size-dependent changes in glutathione metabolism, ferritin levels, and ACSL4 expression.

Audience:

This research will be of interest to specialists in cell death, ferroptosis, redox biology, and cancer biology. It also holds relevance for aging researchers and translational scientists exploring ferroptosis-based therapies. The findings may influence how cell size heterogeneity is considered in therapeutic design, particularly in oncology and senescence-targeting strategies.

Comments on revised version:

We have no additional comments after revision. Thank you for addressing our initial queries.

https://doi.org/10.7554/eLife.111544.1.sa2

Reviewer #3 (Public review):

In this manuscript, Zatulovskiy and colleagues elaborate on their previous work describing cell size-dependent changes in the proteome by investigating whether these changes can be correlated in differences in cell physiology. Using a cleverly-designed high throughput screen, they searched for compounds that differently-sized cells display differential sensitivity towards. Their primary hit, Era2, is involved in the ferroptosis pathway and serves as the starting point for a detailed study of how excess cell size protects cells from ferroptosis-induced cell death via: 1) lower concentrations of ACSL4 (which produces peroxidation-prone PUFAs), 2) increased ferritin concentrations, and 3) increased GSH concentrations.

Overall, the experiments in this manuscript are well-designed and interpreted. It is an extremely well-written manuscript with a clear trajectory of logic.

Comments on the revised version:

The authors have addressed my original concerns adequately. I do not need to see it again, if there are further revisions.

https://doi.org/10.7554/eLife.111544.1.sa1

Author response:

> ***General Statements***

We were pleased to see that all three reviewers support publication after revision. No one questions the premise that cell size influences ferroptosis susceptibility. The main concerns fall into two categories: (A) disentangling "Cell size vs cell cycle", which is the biggest issue for Reviewer #1 and partially for #3. (B) Additional mechanistic tests including SLC7A11 and ferritin functional tests (Reviewer #2) and lysosomal iron (via LysoRhoNox) and some further ACSL4 experiments (Reviewer #3). Other reviewer concerns are more minor.

In our revision, we have addressed the reviewer's specific criticisms with additional experiments as described below. We believe the constructive feedback from peer reviews helped us to significantly extend our mechanistic findings and strengthen the manuscript through revision.

> ***Point-by-point description of the revisions***
>
> ***Reviewer #1****:*
>
> *Summary:*
>
> *The study by Zatulovskiy et al. examined how cell size influences cell susceptibility to ferroptosis. The authors found a size dependence specifically for ferroptosis-inducing drug Era2, but not for other drugs. Using various human cell lines (HMEC, HT 1080, RPE 1), the authors generated populations of small and large G1 cells by FACS, CDK4/6 inhibition (palbociclib), or inducible cyclin D1 knockdown, and measured cell susceptibility to ferroptosis. Larger cells were more resistant than smaller cells. Mechanistically, larger cells showed reduced plasma membrane lipid peroxidation, higher glutathione concentrations, and changes in relevant cellular proteins levels, as analyzed using previously published data. Deleting ACSL4, which is involved in ferroptosis, partly eliminated the size dependence of ferroptosis. The work concludes that cell size is a key determinant of ferroptosis susceptibility.*
>
> *My major concerns about this work focus on whether many of the results reflect cell size or cell cycle effects, and whether the FACS-based size-scaling analyses have some misleading features to their design & presentation. If these concerns can be addressed with new experiments, then the conclusions of this paper are justified. If these concerns cannot be addressed, then the authors should more directly acknowledge the alternative hypothesis that cell cycle effects may explain many of their results.*
>
> *The experiments seem to be replicated sufficiently, and most conclusions rely on data from multiple cell lines. My minor comments focus on needs to provide statistics and method details, and on suggestions on how to improve text clarity, but these edits are easily done and don't require new experiments. Overall, this is an interesting study, and it should be published once the concerns below are addressed.*
>
> *Major comments:*
>
> *In experiments reported in Fig 1 and 2A, the authors sort small and large cells in G1, plate them, and later start the drug treatments & cell monitoring. Are these cells actively*

> *cycling (progressing in the cell cycle), and how fast? The large cells are likely to enter S phase earlier than the small cells, so by the time that the authors start their drug treatments, they may be comparing cells in different cell cycle stages, which could influence drug sensitivity more than cell size (as the authors also suggest later in Fig 2). This needs to be controlled for.*
>
> *Furthermore, even if the cells remain in G1 after sorting until the drug treatments are started, the authors should address the fact that the drugs are present for a long time, thus targeting the cells in various cell cycle stages.*

We agree with the reviewer that the cell cycle stage could affect ferroptosis susceptibility and could be a confounding effect in asynchronous cells. One of us (Dixon) reported the cell cycle effects on ferroptosis previously, and we observe them in this manuscript too (Fig. 2B,C,E). We now state this more clearly both in the Results and in the Discussion sections, where we write:

Line 159: "We note that non-arrested cells had a lower susceptibility to Era2-induced ferroptosis compared to cells that were arrested in G1 for 2-3 days, despite being smaller in size. This is likely due to the difference in the fraction of cells in different cell cycle phases between arrested and non-arrested conditions since cells in S/G2/M phases are known to be more resistant to ferroptosis than cells in G0/G1 phases (Rodencal et al, 2024; Kuganesan et al, 2023)"

Line 533: "Cells in G1 phase of the cell cycle were reported to be more susceptible to ferroptosis (Rodencal et al, 2024; Kuganesan et al, 2023), which suggested that ferroptosis inducers could be used in combination with cancer drugs, like the CDK4/6 inhibitor palbociclib, that arrest cells in G1 phase of the cell cycle (Herrera-Abreu et al, 2024). However, while CDK4/6 inhibitors arrest cells in G1, they do not inhibit cell growth, such that the longer they are arrested, the larger the cells grow (Lanz et al, 2022; Crozier et al, 2023; Manohar et al, 2023). This results in a complex, nonmonotonic ferroptotic response dynamics in cells treated with CDK4/6 inhibitors (Fig. 2B,E). Just following CDK4/6 inhibitor treatment, as more and more cells are arrested in G1 phase, cells become more sensitive to both RSL3- and erastin-induced ferroptosis (Kuganesan et al, 2023; Rodencal et al, 2024). However, the longer the cells are arrested, the larger they become, which further promotes their susceptibility to RSL3 (Fig. S1B) but reduces their susceptibility to Era2-induced ferroptosis (Fig. 2B). The fact that the cell cycle arrest and cell size increase have opposing effects on Era2-induced ferroptosis susceptibility could explain why different studies reported seemingly contradictory results, where sometimes an increased and sometimes a decreased or unchanged sensitivity to system x_c^- inhibitors was observed depending on the cell type, duration and type of cell cycle arrest (Lee et al, 2024; Kuganesan et al, 2023; Rodencal et al, 2024). Such complex interplay between the cell cycle and cell size effects on ferroptosis suggests that combination therapies utilizing CDK4/6 inhibitors and ferroptosis inducers would have to carefully choose a dosage schedule."

Given the potentially confounding effects of the cell cycle in cycling cells sorted by size, we performed an additional experiment, in which RPE-1 cells were pre-treated with the CDK4/6 inhibitor palbociclib to synchronize them in G1 phase prior to treatment. These cells were then continuously exposed to palbociclib during the Era2 treatment (Fig. 2C-E). RPE-1 cells pretreated with palbociclib for 2 and 4 days had the same cell cycle distribution with 94% of cells being arrested in G1, but with different sizes. Cells treated with palbociclib for 4 days were significantly larger and more resistant to Era2.

Additionally, in the experiment shown in Fig. 5E,F, where we FACS-sorted *WT* and *ACSL4 KO* HMEC cells by cell size, and then measured Era2 susceptibility, we pre-treated the cells with palbociclib for 24 h to synchronize them in G1 prior to the sorting. We then cultured the cells in the presence of palbociclib during the Era2 treatment to avoid the cell cycle effects

observed in Fig. 2. In this case, we still observe that larger cells are more resistant to Era2, consistent with our conclusion that cell size protects against Era2-induced ferroptosis.

> *Can the G1 arrest-driven changes in drug susceptibility (Fig 2 C-D) be attributed to cell size? Can the authors rescue the palbociclib treatment with rapamycin or other growth inhibitors that allow size to remain small during G1 arrest?*

We have attempted to perform these experiments, but when we co-treated the cells with palbociclib and mTORC inhibitors, but observed variable results, which are likely due to the fact that prolonged mTORC inhibition itself rewires cellular metabolism and reduces cell susceptibility to ferroptosis, as one of us (Dixon) found previously (Armenta et al. (2022), Ferroptosis inhibition by lysosome-dependent catabolism of extracellular protein. Cell Chemical Biology 29: 1588-1600.e7). Our results were consistent with this previous report and is now included in a new supporting figure panel (Fig. S3C):

Thus, upon palbociclib+rapamycin co-treatment there seems to be a competition between cellsize-mediated and metabolism-mediated effects of mTORC inhibition on ferroptosis, which leads to variable outcomes.

> *In Fig 2E-F, is the cell cycle distribution of the samples influenced by CCND1 shRNA induction? Are the drug sensitivity effects due to cell size or cell cycle changes?*

The CCND1 manipulation model is extensively characterized in our recent work cited in this manuscript (You et al. (2025), Cell size-dependent mRNA transcription drives proteome remodeling. 2025.10.30.685141 doi:10.1101/2025.10.30.685141). Indeed, CCND1 shRNA cells have a slightly elongated G1 phase due to a ~30% reduction in Cyclin D1 concentration: the G1 fraction changes from ~70% in wild-type to ~80% in CCND1 shRNA cells, which could potentially affect the ferroptosis susceptibility, but the additional results obtained on synchronized RPE-1 cells, described above (Fig. 2C-E), support the conclusion that the primary effect on Era2 sensitivity is due to cell size.

> *Can the authors address the meaningfulness of the FACS-based size-scaling results in cases where cell-to-cell variability is very large? For example, in Fig 4D&G, the results are so variable even in identically sized cells that the importance of the size-scaling pattern seems questionable.*

We do observe variability in fluorescent probe-based measurements of GSH and lipid oxidation, which could be due to biological (natural cell heterogeneity) and/or technical (low sensitivity of the probes) reasons. However, when we look at binned data and compare the mean values ± s.e.m. for each bin, we observe a robust and reproducible trend (black line with dark-grey shaded area), even though the SD is quite broad (lighter shaded area). We believe such trends are meaningful when describing cell death in probabilistic terms as we do. I.e., the GSH measurement might not be precise enough to predict cell death for a given individual cell, but the statistical trend is clear and these measurements help predict cell death probabilities for cells of different sizes.

> *In Figs 4B-D, the cell size axis seems to have over 4-fold size variability, but when the authors show the analysis of this data (Figs 4E-G) the variability is only 2-fold. What was excluded and on what basis?*

To address this point, we have now clarified in the Methods section how the data were processed and what data points we excluded from this analysis:

Line 671: “For all binned flow cytometry data plots, the cells below the 2nd and above the 98th cell size percentiles were excluded to remove the extreme outliers. Then, the remaining data were binned by size and plotted as background-corrected average fluorescence intensity

for each bin against the bin's average cell size. Bins with fewer than 200 cells were excluded from the analysis to reduce noise."

Typically, such pre-processing reduces the size range, mostly from the large-cell end, because of the long right tail of the size distribution containing a few very large cells.

> *Based on the methods section & figure legends of Fig 4B-I, the RPE cells were not pre-sorted to include only G1 cells, nor did the assay account for cell cycle differences. How can these data be used to explain results from earlier figures, where analyses were exclusively focused on size differences in G1?*

This is a valid point: Cells in the GSH measurement experiment were not gated by Hoechst signal for G1 phase because the channel normally used for Hoechst staining was in this case occupied by the MCB probe. However, given the data in Fig. 4A,B showing that the GSH production machinery is superscaling when measured specifically in G1-phase cells, we believe the flow cytometry data in Fig. 4C-J showing GSH concentration increasing with cell size across the whole cell cycle is very likely true for G1 cells as well.

> *Minor comments:*
>
> *I recommend clarifying in the early introduction that all size changes discussed are in the absence of DNA content increase."*

We have now clarified this in the introduction (Line 41 and Line 81).

> *The introduction seems to cite primary research and review paper in the same sentences, which is a bit misleading as the reviews don't seem to add new evidence.*

We have removed review citations where they did not provide additional context.

> *OPTIONAL*
>
> *In the second introduction paragraph, consider the classification/description of the three different mechanisms. Currently, it seems that these mechanisms are not independent of each other, and the details provided about each mechanism are inconsistent."*

We have now modified this paragraph to make the description more consistent.

> *Please provide statistics for the IC50 values reported based on Fig 1C. Were small and large cells statistically different? Are the IC50 values reported as +/- standard deviation or some other metric?*

This has now been clarified in the text as follows:

"For example, at the 72 h time point, the Era2 IC50 was 28 ± 11 μM (mean ± SD) for large cells versus 2.0 ± 1.4 μM for small cells (Student's t-test: $p = 0.039$) (Fig. 1C)."

> *Providing more insight into why Era2 and RSL3 treatments yield more opposite responses would be of great interest to the field."*

We agree this is an important point that should be discussed in more detail. In the field of ferroptosis, context-dependent (i.e., cell type-specific) effects are common and multiple groups including our own (Dixon) have published extensively on genes and mechanisms that can lead to differences between erastin2 and RSL3 sensitivity. For example, there are studies showing that the mTOR pathway or the p53 pathway can either prevent or promote ferroptosis, depending on the cell type and/or other currently unknown variables. To address more specifically the differences between Era2 and RSL3 in the context our observed cell-sizedependent response, we have now added more data and discussion. In the Results section we added panel 4B and the following text:

Line 359: “While the upregulation of GSH biosynthesis may promote the resistance of larger cells to ferroptosis, such an upregulation alone cannot explain why larger cells become more resistant to ferroptosis induced by the cystine import inhibitor Era2, but not, for example, by the GPX4 inhibitor RSL3 (Chan et al, 2025) (Figs. 2B, S1B). We found previously that upon mTORC1 inhibition cells can evade cystine deprivation-induced ferroptosis by uptake and catabolism of cysteine-rich extracellular proteins, mostly albumin (Armenta et al, 2022) (Fig. S3C). This process involves albumin degradation in lysosomes, predominantly by cathepsin B (CatB), and subsequent export of cystine from lysosomes to fuel the synthesis of glutathione. Large cells undergo proteome rearrangements similar to those occurring upon mTORC1 inhibition (Zatulovskiy et al, 2022). This suggests that large cells may upregulate CatB expression to bypass the Era2-induced cystine import inhibition via system xc-. To test this hypothesis, we used flow cytometry to measure how the expression of cathepsin B and the system xc- cystine/glutamate transporter SLC7A11 (xCT) scales with cell size (Fig. 4B). We found that SLC7A11 concentration modestly decreases, while CatB concentration significantly increases with cell size (Fig. 4B). This shift in the ratio between SLC7A11 and CatB supports the hypothesis that larger cells may rely less on cystine import via system xc- and thus become more resistant to system xc- inhibition by Era2.”

Additionally, in the Discussion we added the following:

Line 578: “We show that large cells may become resistant specifically to Era2 but not RSL3 through the upregulation of lysosomal function, particularly cathepsin B expression, which enables the uptake and catabolism of cysteine-rich extracellular proteins. A size-dependent shift in the ratio between SLC7A11 and cathepsin B makes large cells less dependent on cystine import via system xc-, and thus, more resistant to Era2. In addition to this, it was reported that RSL3 can induce ferroptosis independently of GPX4 and may target other selenoproteins (DeAngelo et al, 2025; Cheff et al, 2023), which could also contribute to the difference in sizedependent responses to RSL3 and Era2.”

> *Is the BODIPY-C11 labeling specific to plasma membrane, as suggested by the writing of the authors, or do the results shown integrate signals over all cell membranes?*

We thank the reviewer for pointing this out. BODIPY-C11 581/591 stains many membranes in the cell, not just the plasma membrane. We have changed the wording in the manuscript to reflect this.

> *How exactly is gating done for the flow cytometry samples? Especially when analyzing size-scaling, the results are likely to be sensitive to outliers, such as those seen in Fig 4C (a subpopulation of very low CFSE stained cells). Can the authors clarify their methods and/or display supplementary figures with gating examples?*

We have now specified our gating strategy in the Methods section (Line 663) and added a corresponding Supplementary Figure S5.

> *In Fig 4, total protein staining was used as a control, whereas Fig 5B b-actin was used as a control. Why did the authors rely on different controls approaches for essentially the same measurements? Are these controls comparable?*

In our flow cytometry experiments, we consistently use live-cell total protein stain (CFSE) for live cells, and anti-Tubulin immunofluorescent staining for fixed cells, both of which scale in proportion to cell volume and act as a read-out for total cellular protein content (Lanz and Zatulovskiy et al., Mol Cell 2022; Berenson et al. MBoC 2019), which we use to calculate concentrations of other cellular components (analogous to loading controls). In Fig. 5B, betaActin is used as a reference - a protein whose concentration does not change with cell size, as opposed to ACSL4 whose concentration decreases with cell size. In this plot, both ACSL4 and beta-Actin amounts were normalized to alpha-Tubulin, which is analogous to a

concentration calculation using loading control. This is now explained in more detail in the Figure legend.

> ***Reviewer #1 (Significance):***
>
> *I work in the cell size research field, and I am familiar with other related works in this field. My evaluation reflects a specialist's view of this study. Overall, this study will be of a large interest to a small group of specialists, and specific aspects of the work will also gain some interest from broader basic research audiences studying mechanisms of drug responses and ferroptosis in general. However, I do not see this work gaining very broad interest across larger audiences, simply because the field of cell size research is not of broad interest, and this is not a landmark study for the field.*
>
> *The field of cell size research has long searched for size-dependent functions, as these could help explain why cell size matters. This study is a nice addition to our field, helping establish ferroptosis as a size-dependent function. However, the significance of this work relies on how clearly the authors can establish that their results are cell size rather than cell cycle effects (see major comments above). Should the authors address these concerns, then this study will provide some conceptual and mechanistic insight.*
>
> *Regarding mechanistic insights, this work is in stark contrast to a recent study about sizedependency of ferroptosis (https://doi.org/10.1016/j.isci.2025.112363), where increased cell size heightened sensitivity to the GPX4 inhibitor RSL3, thus suggesting an opposite conclusion than what the authors observed with the drug Era2. The authors examined this contradiction, and while their results with the drug RSL3 agreed with the recent study, they did not explain why different drug mechanisms yield opposite results. Providing more insights into this discrepancy would increase the impact of this work.*
>
> *Regardless of the impact of this work, I want to emphasize that I am fully supportive of seeing this work published once the technical concerns have been addressed. Our field will benefit from this work, and this work could catalyze important future research. The general topic studied here has the potential to become very important.*

We thank the reviewer for their thoughtful assessment and for supporting publication pending resolution of the technical concerns. We respectfully disagree that our audience is likely narrow: Reviewer #2 noted broad relevance to specialists in cell death/ferroptosis, redox biology, cancer biology, aging, and translational efforts in ferroptosis-based therapies, and Reviewer #3 similarly emphasized both cell size and ferroptosis/cell death communities. We therefore believe the work will be of interest across multiple active fields, particularly because it highlights how cell size heterogeneity can shape drug response.

We agree that the significance hinges on clearly distinguishing cell size from cell-cycle effects, and we have strengthened the corresponding controls/analyses and adjusted language accordingly (see responses to major comments above). We also addressed the reported discrepancy between Era2 and RSL3 size-dependencies by adding new data (Fig. 4B) and expanded discussion. We very much hope that the reviewer appreciates the efforts we have made to strengthen this manuscript and resolve the technical concerns. For these reasons, we believe this work will have an impact on several fields and gain a broad readership.

> ***Reviewer #2****:*
>
> *Zatulovskiy et al. demonstrate that cell size modulates susceptibility to ferroptosis, a form of iron-dependent cell death driven by lipid peroxidation. Using human cell lines (HMEC, HT-1080, RPE-1), the authors examined cell size through FACS sorting, CDK4/6 inhibition and inducible cyclin D1 knockdown. They found that larger cells are more resistant to ferroptosis induced by system xc^{-} inhibition (erastin2), but more sensitive to GPX4 inhibition (RSL3), highlighting pathway-specific size dependencies.*

Mechanistically, larger cells exhibited:

- Higher glutathione levels, supporting lipid peroxide detoxification

- Increased ferritin expression, promoting iron sequestration

- Lower ACSL4 levels, reducing incorporation of peroxidation-prone lipids

These findings were supported by high-throughput microscopy, flow cytometry (BODIPY-C11 lipid peroxidation assays), and proteomic analyses. The study concludes that cell size influences proteome composition and metabolic capacity, thereby shaping cell death decisions, an insight with implications for aging, cancer, and ferroptosis-based therapies.

Major Comments

(1) Direct evaluation of SLC7A11 abundance and function is needed

The opposite size-dependent effects of erastin2 and RSL3 strongly suggest a role for SLC7A11/system xc⁻ activity in size-dependent ferroptosis resistance. However, SLC7A11 levels were not quantified due to insufficient peptide detection in the proteomic data. o Direct measurement of SLC7A11 protein levels (immunoblotting or flow cytometry) in small vs large cells would test whether its expression scales with size.

a) Functional perturbation (siRNA/CRISPR knockdown) followed by erastin2 treatment would provide mechanistic validation. o Use of additional SLC7A11 inhibitors (e.g., sulfasalazine, sorafenib) could further test whether the size resistance phenotype is xc⁻-specific.

We agree that the difference in size-dependent responses to RSL3 and Era2 is an important point that needs further investigation and discussion, as other reviewers also pointed out. To address more specifically the differences between Era2 and RSL3 in the context of cell-sizedependent response, we have now added more data and discussion. In the Results section we added panel 4B measuring SLC7A11 and Cathepsin B scaling with cell size and the following text:

Line 359: “While the upregulation of GSH biosynthesis may promote the resistance of larger cells to ferroptosis, such an upregulation alone cannot explain why larger cells become more resistant to ferroptosis induced by the cystine import inhibitor Era2, but not, for example, by the GPX4 inhibitor RSL3 (Chan et al, 2025) (Figs. 2B, S1B). We found previously that upon mTORC1 inhibition cells can evade cystine deprivation-induced ferroptosis by uptake and catabolism of cysteine-rich extracellular proteins, mostly albumin (Armenta et al, 2022) (Fig. S3C). This process involves albumin degradation in lysosomes, predominantly by cathepsin B (CatB), and subsequent export of cystine from lysosomes to fuel the synthesis of glutathione. Large cells undergo proteome rearrangements similar to those occurring upon mTORC1 inhibition (Zatulovskiy et al, 2022). This suggests that large cells may upregulate CatB expression to bypass the Era2-induced cystine import inhibition via system xc-. To test this hypothesis, we used flow cytometry to measure how the expression of cathepsin B and the system xc- cystine/glutamate transporter SLC7A11 (xCT) scales with cell size (Fig. 4B). We found that SLC7A11 concentration modestly decreases, while CatB concentration significantly increases with cell size (Fig. 4B). This shift in the ratio between SLC7A11 and CatB supports the hypothesis that larger cells may rely less on cystine import via system xc- and thus become more resistant to system xc- inhibition by Era2.”

Additionally, in the Discussion we added the following:

Line 578: “We show that large cells may become resistant specifically to Era2 but not RSL3 through the upregulation of lysosomal function, particularly cathepsin B expression, which

enables the uptake and catabolism of cysteine-rich extracellular proteins. A size-dependent shift in the ratio between SLC7A11 and cathepsin B makes large cells less dependent on cystine import via system xc^-, and thus, more resistant to Era2. In addition to this, it was reported that RSL3 can induce ferroptosis independently of GPX4 and may target other selenoproteins (DeAngelo et al, 2025; Cheff et al, 2023), which could also contribute to the difference in sizedependent responses to RSL3 and Era2."

> *(2) Functional tests of ferritin contribution to resistance are needed Although elevated ferritin (FTH1/FTL) levels in larger cells represent a strong correlational signal, definitive experimental evidence establishing causality is currently lacking. o Measuring the labile iron pool directly in size-stratified populations would strengthen the link. o Knockdown of FTH1 or FTL could reveal whether ferritin upregulation is necessary for the resistance of large cells to ferroptosis.*

We thank the reviewer for raising this point. We have now completed additional experiments, as suggested by the reviewer, and found that iron chelation is unlikely to mediate the sizedependent response to Era2. We have modified the manuscript accordingly and added the following data and discussion to address this point:

Line 296: "The observed increase in ferritin concentration with cell size could therefore lead to additional Fe^{2+} ion chelation, which in turn would protect large cells from iron-dependent lipid peroxidation and ferroptosis. However, when we measured the concentration of labile intracellular Fe^{2+} using a fluorescent probe FerroOrange (Hirayama et al, 2020), we did not observe any size-dependent decrease in labile iron concentration (Fig. S2A). Previous work suggests a link between increased sequestration of ferrous iron in lysosomes and resistance to ferroptosis. It was reported that senescent cells, which are also large (Fig. S3A,B), gain resistance to ferroptosis through lysosomal alkalinization and sequestration of ferrous iron in lysosomes (Loo et al, 2025). We therefore tested whether the superscaling of lysosomes observed in large cells (Lanz et al, 2022; You et al, 2025) promotes Era2 resistance through lysosomal iron sequestration. To do this, we stained the cells with the lysosomal iron detection probe Lyso-FerroRed (Saimoto et al, 2025) and measured its scaling using flow cytometry (Fig. S2B). We observed that the amount of Lyso-FerroRed, and therefore, the amount of lysosomal iron, scaled in direct proportion to cell size, just like the total cellular protein content (Fig. S2B). These results indicate that iron chelation by ferritin and its sequestration in lysosomes are unlikely to play a crucial role in size-dependent decrease in Era2 sensitivity."

> *(3) Relevance to senescence should be addressed experimentally or explicitly discussed*
>
> *Given that senescent cells are enlarged and accumulate in aged and tumour tissues, testing senescent models for erastin2 resistance would greatly strengthen the physiological significance."*

We agree that an increase in cell size contributing to the resistance of senescent cells to ferroptosis is intriguing. We have now added a Supplementary Figure S3 and discussion of this point in the manuscript as follows:

Discussion line 552: "…our data suggest that previously reported resistance of senescent cells to ferroptosis can at least partially be due to the increased cell size, a well-established hallmark of senescence."

> *Minor Comments*
>
> *(1) Mechanistic nuance regarding RSL3 should be included*
>
> *RSL3 has been reported to induce ferroptosis independently of GPX4 (PMID: 37087975, PMID: 40392234) and may target other selenoproteins such as TXNRD1. This nuance*

> *would help explain the observed divergence between RSL3 and erastin2 sensitivity across sizes.*

We have now added this in the Discussion as suggested by the reviewer (line 583):

"In addition to this, it was reported that RSL3 can induce ferroptosis independently of GPX4 and may target other selenoproteins (DeAngelo et al, 2025; Cheff et al, 2023), which could also contribute to the difference in size-dependent responses to RSL3 and Era2."

> *(2) Dynamic range of BODIPY-C11 assays needs commentary*
>
> *Despite high erastin2 doses, the oxidized BODIPY signal remains close to DMSO levels. The authors should comment on whether this reflects high GSH buffering capacity, probe limitations, or other factors."*

We believe there are both technical (narrow dynamic range of the probe) and biological reasons for the relatively small (2-3 fold) difference in Oxidized-to-Non-oxidized BODIPY-C11 ratios between DMSO and Era2-treated cells. The biological reason is that the cells continue producing GSH until they fully deplete the cystine pool, which happens ~20-24 h after Era2 addition. Once the cystine pool is depleted, the cells very rapidly deplete GSH and initiate cell death. Therefore, there is only a short time window where cells are strongly depleted of GSH before dying. We see this small fraction of cells with a high Oxidized BODIPY-C11 signal in our flow cytometry experiments and in previous microscopy analysis of BODIPY-C11 (Murray et al., Protocol for detection of ferroptosis in cultured cells. STAR Protoc. 2023), but at our chosen time point (20h Era2) most cells are not as bright because we aimed to analyze the population before the onset of widespread cell death.

> *(3) Western blot for shCycD1 depletion should be included*
>
> *CycD1 depletion usually causes cells to stop proliferating, which is not the case here. Therefore, depletion must be partial. The level of depletion should be shown by immunblotting."*

The CCND1 manipulation model is extensively characterized in our recent work cited in this manuscript (You et al. (2025), Cell size-dependent mRNA transcription drives proteome remodeling. 2025.10.30.685141 doi:10.1101/2025.10.30.685141). CCND1 shRNA cells do not fully arrest in G0/G1 because the concentration of Cyclin D1 protein in this system is only partially decreased, as the reviewer noted. As a result, the cells have a slightly elongated G1 phase due to a ~30% reduction in Cyclin D1 concentration, but continue to proliferate. The G1 fraction changes from ~70% in wild-type to ~80% in CCND1 shRNA cells.

> ***Reviewer #2 (Significance):***
>
> *General Assessment: This study presents a mechanistic link between cell size and ferroptosis susceptibility. Using high-throughput microscopy, proteomics, and genetic perturbations across multiple human cell lines, the authors demonstrate that larger cells are more resistant to ferroptosis induced by system xc^- inhibition (erastin2). This resistance is attributed to elevated glutathione production, increased ferritinmediated iron sequestration, and reduced ACSL4-dependent lipid peroxidation. The experimental design is rigorous and multifaceted, with consistent results across cell types and size manipulation methods. While the study is limited to in vitro systems, its conceptual and mechanistic insights lay the groundwork for future in vivo and translational investigations.*
>
> *Advance: This work is the first to systematically show that cell size directly influences ferroptosis susceptibility via proteome scaling. It reconciles previous findings that large cells are sensitized to GPX4 inhibition (RSL3) by demonstrating that the ferroptosis*

> *pathway targeted system xc⁻ vs GPX4 determines the direction of size-dependent vulnerability. The study provides a conceptual advance by positioning cell size as a regulatory axis in cell death decisions, and a mechanistic advance by identifying size-dependent changes in glutathione metabolism, ferritin levels, and ACSL4 expression.*
>
> *Audience: This research will be of interest to specialists in cell death, ferroptosis, redox biology, and cancer biology. It also holds relevance for aging researchers and translational scientists exploring ferroptosis-based therapies. The findings may influence how cell size heterogeneity is considered in therapeutic design, particularly in oncology and senescence-targeting strategies.*
>
> *Field of Expertise: Translational cancer biology, cell cycle regulation, proteomics, therapy resistance, molecular mechanisms of cell death.*

We thank Reviewer #2 for their careful and constructive assessment of our manuscript. We were happy that they appreciated the rigor of our multifaceted approach. We are also grateful for their thoughtful perspective on the conceptual and mechanistic advances, and for highlighting the broader relevance of this work to ferroptosis biology, redox regulation, cancer and aging research.

> ***Reviewer #3 (Evidence, reproducibility and clarity):***
>
> *In this manuscript, Zatulovskiy and colleagues elaborate on their previous work describing cell size-dependent changes in the proteome by investigating whether these changes can be correlated in differences in cell physiology. Using a cleverly-designed high throughput screen, they searched for compounds that differently-sized cells display differential sensitivity towards. Their primary hit, Era2, is involved in the ferroptosis pathway and serves as the starting point for a detailed study of how excess cell size protects cells from ferroptosis-induced cell death via: 1) lower concentrations of ACSL4 (which produces peroxidation-prone PUFAs), 2) increased ferritin concentrations, and 3) increased GSH concentrations.*
>
> *Overall, the experiments in this manuscript are well-designed and interpreted. It is an extremely well-written manuscript with a clear trajectory of logic. I have only a few major concerns that should be addressed before publication:*

We thank Reviewer #3 for their careful reading of the manuscript and for the clear summary of our study and its central findings. We appreciate their positive assessment of the experimental design, interpretation, and overall clarity of the writing and logical flow. We are also grateful for their constructive feedback and take their major concerns seriously; we have addressed each point in detail below.

> *Major concerns:*
>
> *(1) In Figure 3E, the authors gate their flow cytometry data using SYTOX so that they are only analyzing live cells. Based on their gating scheme, it seems like there are really a lot of dead cells. Presumably the cells that died were the most sensitive to Era2, so it seems an oversight to discard these cells. Of course, it is not appropriate to analyze dead cells, but this could potentially be solved by using a shorter treatment duration than 24 hours wherein fewer cells die."*

This is a good point. To address it, we have now replaced this panel with a time point where most cells are still alive (20 h, 0.2 μM Era2), as suggested by the reviewer (Fig. 3E,F). This did not change the conclusion that BODIPY-C11 oxidation decreases with cell size.

> *(2) In Figure 5, are the small, medium, and large bins for ACSL4 KO cells the same as for WT cells? If the ACSL4 KO cells are just bigger to begin with, this could explain why the*

> *"small" bin has greater cell survival than the WT small bin. Moreover, is the overlap between the three bins the same in the WT and KO cells?*

This is an important point that we now address with data shown in Fig. S4B. We have now added a Supplementary Figure S4B to show the relative size of small, medium, and large *WT* and *ACSL4 KO* HMEC cells. As seen from this graph, the *ACSL4 KO* cells are not bigger than *WT* cells. Importantly, the fold-range between the small and large FACS-sorted cells is similar (~1.9 to 2-fold).

> *(3) Loo, et al. Nat Comms 2025 similarly found that senescent cells (which are enlarged) are resistant to ferroptosis using the same inhibitor as the authors. In contrast to the authors, they show that this is due to lysosomal alkalinization and sequestration of ferrous iron in lysosomes. Given that Lanz et al. 2022 found that lysosomal components super-scale with cell size, it seems like this would be an important hypothesis to address. Free lysosomal iron can be easily measured with the LysoRhoNox stain. Loo et al. was able to restore ferroptosis sensitivity in senescent cells using the V-ATPase activator EN6, so it would be important for the authors to address whether this (or similar) treatment would have the same effect in enlarged cells.*

This is an excellent point. We have now performed this experiment and added it to the manuscript, as suggested by the reviewer. Based on the Lyso-FerroRed staining (another brand name for the LysoRhoNox probe), we do not see an increase in lysosomal iron sequestration in large cells (Fig. S2B):

Line 301: “Previous work suggests a link between increased sequestration of ferrous iron in lysosomes and resistance to ferroptosis. It was reported that senescent cells, which are also large (Fig. S3A,B), gain resistance to ferroptosis through lysosomal alkalinization and sequestration of ferrous iron in lysosomes (Loo et al, 2025). We therefore tested whether the superscaling of lysosomes observed in large cells (Lanz et al, 2022; You et al, 2025) promotes Era2 resistance through lysosomal iron sequestration. To do this, we stained the cells with the lysosomal iron detection probe Lyso-FerroRed (Saimoto et al, 2025) and measured its scaling using flow cytometry (Fig. S2B). We observed that the amount of Lyso-FerroRed, and therefore, the amount of lysosomal iron, scaled in direct proportion to cell size, just like the total cellular protein content (Fig. S2B). These results indicate that iron chelation by ferritin and its sequestration in lysosomes are unlikely to play a crucial role in size-dependent decrease in Era2 sensitivity.”

> *Minor concerns:*
>
> *(1) It would be helpful if this manuscript were re-submitted with line numbers to more easily reference the text.*

We have added line numbers for convenience.

> *(2) In Figure 5A and other figures that reproduce data from Lanz et al. 2022, it would be helpful to have a summary curve for the overall abundance of each protein rather than only the individual peptide curves. These plots (particularly Figure 5A) are difficult to interpret since some peptides were presumably more abundant / measured with higher confidence than others.*

We have added the average ACSL4 protein slope line to Fig. 5A.

> *(3) In Figure 5, the authors show the validation of the ACSL4 KO HT-1080 cell line but not HMEC, even though both are used in this figure. It would be useful to show both. Additionally, the authors switch back and forth between the two cell lines for this figure, and it is not clear why.*

We have added the HMEC *ACSL4 KO* validation Western blot in Fig. S4A.

For the BODIPY oxidation experiment (Fig. 5D), we used HT-1080 instead of HMEC because HT1080 cells are sensitive to lower concentrations of Era2, and therefore, we could better optimize the Era2 concentrations and treatment durations to measure BODIPY oxidation at the time point when most cells are still alive but demonstrate a pronounced oxidized BODIPY signal.

> *(4) In Figure 5B, the authors use antibody-based staining of ACSL4 and flow cytometry to correlate a loss of ACSL4 expression with increased cell size, validating the proteomics data in Figure 5A. This does not seem like a good way to do this. Firstly, fixing cells with formaldehyde alters their size (is this proportional across differently sized cells? It's impossible to know), which makes it inappropriate to use SSC as a proxy for size in this particular situation. Secondly, the normalization scheme here doesn't make sense. If actin was used as a reference protein, why was tubulin used to normalize ACSL4 abundance? Overall, this seems like a very round-about experiment that could have just been addressed by doing a simple western blot with the four size bins sorted from live cells (as it was in the proteomics). If the issue is that ACSL4 is not detectable by western in the HMEC cells, another solution would be plating the live, sorted bins on coverslips and measuring by IF (or using the HT-1080 cells).*

We prefer IF flow cytometry to Western blotting for protein scaling analysis because it is more quantitative and provides cell size and protein content information for each individual cell. While in principle, different-sized cells might change their size differently during fixation, the cells that were larger or smaller prior to the fixation remain larger or smaller after fixation as well.

Therefore, the SSC measurement after fixation still provides reliable information on size ranking, even if SSC does not perfectly linearly scale with cell volume. We do not use the SSC information to calculate protein concentrations here. Instead, we divide the amount of our protein of interest in the cell by the amount of constitutively-expressed Tubulin, which acts as an analogue of a loading control in this experiment. In Fig. 5B, both ACSL4 and Actin were normalized to Tubulin to estimate their concentrations. Actin is used just as a reference protein to show how the concentration of a perfectly scaling protein remains constant across cell size, as opposed to the sub-scaling ACSL4. Tubulin in this case was used as a proxy for total cellular protein content, which scales linearly in proportion to cell volume. This approach for determining the scaling behaviors of different proteins was previously validated in Lanz et al., Mol Cell 2022.

> *(5) In Figure 5E/5F, the authors pre-arrest the cells in G1 with palbociclib before size-sorting them. The pre-arrest is not done in other experiments using this cell line for sizesorting, so it would be important for the authors to comment on why this was done for this experiment but not others."*

As we found in Fig. 2B-E, the cell cycle has confounding effects on size-dependent ferroptosis susceptibility measurements (as discussed in detail in our response to the first major point of Reviewer #1 above). Briefly, to avoid these confounding effects and isolate the effects of cell size from the effects of the cell cycle, we pre-synchronized the cells with 24 h treatment with palbociclib in Fig. 5E,F. This is now better clarified in the text, as follows:

Line 456: "In this experiment, we synchronized cells in G1 phase using palbociclib prior to cell sorting and also incubated the sorted cells in the presence of palbociclib during Era2 treatment to isolate cell size effects from the previously observed confounding effects of the cell cycle on ferroptosis (Fig. 2B,E)."

> *(6) Conceptually, it is difficult for me to understand why large cell size sensitizes cells to GPX4 inhibition but confers resistance to Era2 treatment. Particularly given the pathway described in Figure 3A, I am having trouble understanding why these would convey such opposing phenotypes. Shouldn't the extra ferritin in the bigger cells also help them cope with GPX4 inhibition if, as the authors state in the discussion, the increased sensitivity to the GPX4 inhibitor is reported to be mediated by (among other things) iron accumulation? A deeper discussion of this seeming-incongruity would be helpful for contextualizing the broader role of cell size in determining ferroptosis sensitivity.*

We agree this is an important point, which was also raised by the other reviewers. As such, we note that context-dependent (i.e., cell type-specific) effects are common in the ferroptosis field, and multiple groups including our own (Dixon) have published extensively on genes and mechanisms that can lead to differences between erastin2 and RSL3. For example, there are studies showing that the mTOR pathway or the p53 pathway can both prevent and promote ferroptosis, depending on the cell type or some other hidden variable.

To better address the differences between Era2 and RSL3 in the context of the cell-sizedependent response, we have now added more data and discussion. In the Results section we added panel 4B and the following text:

Line 359: “While the upregulation of GSH biosynthesis may promote the resistance of larger cells to ferroptosis, such an upregulation alone cannot explain why larger cells become more resistant to ferroptosis induced by the cystine import inhibitor Era2, but not, for example, by the GPX4 inhibitor RSL3 (Chan et al, 2025) (Figs. 2B, S1B). We found previously that upon mTORC1 inhibition cells can evade cystine deprivation-induced ferroptosis by uptake and catabolism of cysteine-rich extracellular proteins, mostly albumin (Armenta et al, 2022) (Fig. S3C). This process involves albumin degradation in lysosomes, predominantly by cathepsin B (CatB), and subsequent export of cystine from lysosomes to fuel the synthesis of glutathione. Large cells undergo proteome rearrangements similar to those occurring upon mTORC1 inhibition (Zatulovskiy et al, 2022). This suggests that large cells may upregulate CatB expression to bypass the Era2-induced cystine import inhibition via system xc-. To test this hypothesis, we used flow cytometry to measure how the expression of cathepsin B and the system xc- cystine/glutamate transporter SLC7A11 (xCT) scales with cell size (Fig. 4B). We found that SLC7A11 concentration modestly decreases, while CatB concentration significantly increases with cell size (Fig. 4B). This shift in the ratio between SLC7A11 and CatB supports the hypothesis that larger cells may rely less on cystine import via system xc- and thus become more resistant to system xc- inhibition by Era2.”

Additionally, in the Discussion we added the following:

Line 578: “We show that large cells may become resistant specifically to Era2 but not RSL3 through the upregulation of lysosomal function, particularly cathepsin B expression, which enables the uptake and catabolism of cysteine-rich extracellular proteins. A size-dependent shift in the ratio between SLC7A11 and cathepsin B makes large cells less dependent on cystine import via system xc-, and thus, more resistant to Era2. In addition to this, it was reported that RSL3 can induce ferroptosis independently of GPX4 and may target other selenoproteins (DeAngelo et al, 2025; Cheff et al, 2023), which could also contribute to the difference in sizedependent responses to RSL3 and Era2.”

https://doi.org/10.7554/eLife.111544.1.sa0